약학박사 학위논문

지방간질환에서 핵수용체 NR1D1의 병태생리학적 역할에 대한 연구

The study for pathophysiological roles of NR1D1 in fatty liver disease

2017년 2월

서울대학교 대학원

약학과 병태생리학 전공

나 혜 린

Abstract

The study for pathophysiological roles of NR1D1 in fatty liver disease

Hyelin Na

Department of pathophysiology, College of pharmacy

The Graduate School

Seoul National University

The recent studies of nonalcoholic fatty liver diseases (NAFLD) caused by multiple steps actively involve studies of nuclear receptors which are useful as drug targets. Nuclear receptor subfamily 1, group D, member 1 (Nr1d1) is abundantly expressed in the metabolic tissues and organs such as adipose tissues, skeletal muscle, and liver, and specifically expressed in non-parenchymal cells such as hepatic stellate cells, macrophages, and T cells. Expressions of the Nr1d1 in various tissues and cells reflect its roles and functions, and Nr1d1 has been reported to contribute the adipocyte differentiation, muscle development, gluconeogenesis, inflammation and immune response. However, the role and function of NR1D1 in NAFLD was not clearly addressed. To clarify the role of NR1D1 in hepatic lipid metabolism and to understand the molecular pathogenesis of NAFLD, the

Nr1d1 Δex3/4 mice, in which deletion of *Nr1d1* exons 3 and 4 for a functional disruption was introduced, were generated by crossing *Nr1d1* floxed mice with transgenic Zp3-Cre deleter mice. To induce NAFLD stage, the Nr1d1 Δex3/4 mice were challenged by a high fat diet (HFD), and the metabolic phenotypes that responded to these stimuli were observed. The Nr1d1 Δex3/4 mice displayed severe hepatic steatosis compared to the WT mice, and it resulted from the interaction effect between diet and genotype. In addition, to understand the potential molecular mechanism, the differential gene expression was profiled using microarray, and upstream factors and gene coexpression networks were predicted. Interestingly, neutrophils homeostasis and cAMP signaling pathways were affected by the interaction effect, and they were thought to elevate severity of hepatic steatosis in response of HFD-fed functional disruption of Nr1d1. In addition, CCAAT/enhancer-binding protein alpha and hepatocyte nuclear factor 4 alpha were predicted to tether the function of HFD-responsive Nr1d1 Δex3/4, and *thyroid hormone-responsive* (*Thsrp*) was a potential target gene of HFD-responsive Nr1d1 Δex3/4. Taken together, loss of transcriptional function of Nr1d1 was associated with deterioration in hepatic steatosis. The interaction between the *Nr1d1* Δex3/4 genotype with an HFD might mediate these phenotypic changes, probably through a nonclassical transcriptional function of Nr1d1.

Keywords: nuclear recptor, Nr1d1, NAFLD, Cebp*α*, Hnf4*α*, Thrsp
Student Number: 2009-30461

Contents

List of Tables

List of Figures

1. Introduction

1.1. Background

1.1.1. Definition of nonalcoholic fatty liver diseases (NAFLD)

Because the liver is the central organ for energy metabolism and immune system, abnormal regulation of hepatic functions causes nonalcoholic fatty liver diseases (NAFLD), initiated by the accumulation of cytoplasmic triglycerides in more than 5% of hepatocytes, or 55 mg/g liver tissue [Szczepaniak et al., 2005; Hardy et al., 2016]. In detail, the spectrum of NAFLD encompasses three main forms of liver injury: fatty change (steatosis), hepatitis and cirrhosis (Figure 1).

Simple liver steatosis has been thought to be the primary benign state of liver injury, and results from the uncontrolled hepatic fat retained by overnutrition, increased lipogenesis, and enhanced lipolysis in adipose tissue. This abnormality enhanced by genetic predisposition can stimulate endoplasmic reticulum stress, mitochondria dysfunction and inflammation, inducing the liver injury. With the presence of hepatocellular injury plus inflammation and scarring, simple liver steatosis deepens into nonalcoholic steatohepatitis (NASH) [Cohen et al., 2011]. Scarred tissue in the liver replaces the healthy hepatocytes on the stage of fibrosis or/and cirrhosis, ultimately preventing the liver from functioning properly [Tsochatzis et al., 2014]. In spite of sequential development of liver diseases, the progress of NASH can stop, and reverse on the simple liver steatosis, or its own healthy liver state [Hardy et al., 2016].

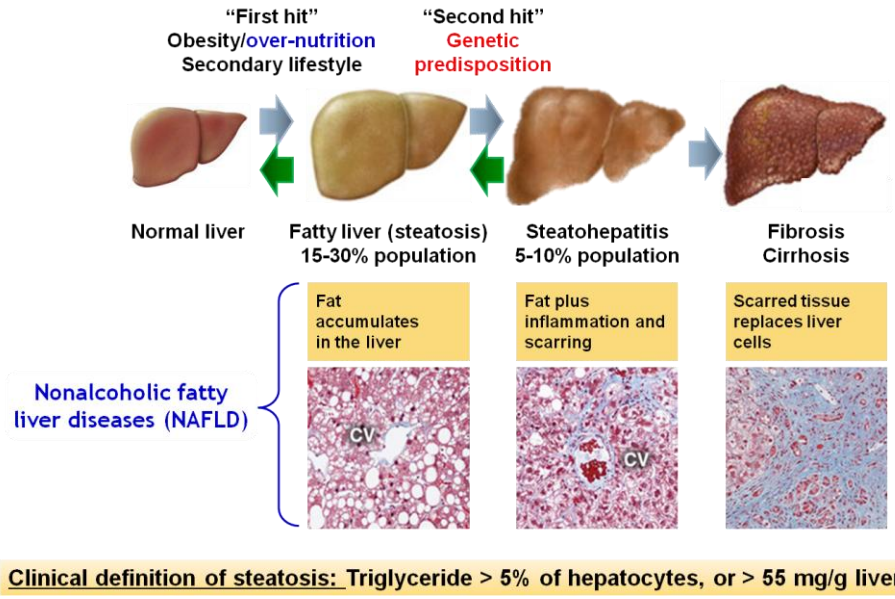

Figure 1. The spectrum of liver diseases reflects the retention of uncontrolled fat.

The spectrum of NAFLD includes simple steatosis, NASH, and cirrhosis. The first hits, as risk factors such as obesity, hepatopathogenic diet, insulin resistance and adipose tissue lipolysis lead to accumulation of triglycerides. This abnormality can stimulate the second hits such as lipotoxicity, ER stress, mitochondria dysfunction and inflammation, promoting NASH and fibrosis.

1.1.2. Association between NAFLD and chronic metabolic syndromes

NAFLD is strongly associated with chronic metabolic syndromes such as type II diabetes mellitus (T2DM), hyperlipidemia, and cardiovascular diseases, and has been regarded as the liver indication of the metabolic syndromes. With the increasing prevalence of obesity and insulin resistance, NAFLD has become the most frequent cause of liver dysfunction worldwide [Hardy et al., 2016]. It is thought that deteriorated metabolic risk factors worsen the progression of NAFLD. Besides, NAFLD affect several extra hepatic organs like heart, kidney, and colon, increasing risk of chronic disease [Armstrong et al., 2014]. Epidemically, global population is estimated at 10-45% as NAFLD patients, and the rates of NAFLD are rapidly increasing in developed countries as well as western countries [Younossi et al., 2016]. Despite the complication and the prevalence of NAFLD, the pathogenesis of NAFLD remains incompletely understood.

1.1.3. Nuclear receptors as therapeutic targets for NAFLD

Since the mechanism of the pathogenesis of NAFLD is unclear, any approved NAFLD treatment except lifestyle modifications including weight reduction diets and exercise was not yet available. They can improve the function of liver and delay the progression of NAFLD. In addition, the T2DM drugs such as pioglitazone and metformin and the antioxidant vitamin E are

considered for NAFLD patients. However, the pioglitazone and vitamin E have some safety issues such as increased risk of bladder cancer and heart failure with pioglitazone, and increased risk of bleeding with vitamin E, and are not sufficient for all NAFLD patients [Lassailly et al., 2016].

To overcome the problems of drugs for NAFLD and meet the unmet needs in NAFLD drugs market, new therapies with strong experimental evidence about various mechanism of action are currently in clinical development [Lassailly et al., 2016] (Table 1). Two promising agents which have entered phase III clinical trial for NAFLD targets nuclear receptors, farnesoid X receptor (FXR) and dual peroxisome proliferator-activated receptor (PPAR) α/δ. Like these, recent many researches for NAFLD involves the nuclear receptors which play key roles in the regulation of metabolism and inflammation, and can mediate the pathogenesis of NAFLD [Wagner et al., 2011].

Nuclear receptors are ligand-activated transcription factors that consist of a DNA-binding domain (DBD) and a ligand-binding domain (LBD). Binding of selective activating ligands to LBD promotes binding of DBD to the specific target sequences, resulting in regulation of target gene expression [Marciano et al., 2014] (Figure 2). Thus, introduction of nuclear receptors are eligible to understand the molecular mechanism in the pathogenesis of NAFLD and provide a novel pharmacological target in NAFLD treatment.

Table 1. Selective NAFLD agents in development

Drug	Modes of action	Clinical trial
Obeticholic acid (OCA/Ocaliva)	FXR agonist and semi-synthetic bile acid analogue	Phase III
Elafibranor (GF-505)	PPARα/δ agonist	Phase III
Aramchol	Synthetic fatty acid-bile acid conjugate	Phase II/III
Emricasan (IDN-6556)	Caspase inhibitor	Phase II
Simtuzumab (GS-6624)	Anti-LOXL2 monoclonal antibody	Phase IIb
GR-MD-02	Galectin 3-inhibitor	Phase II
GS-4997	MAPK5 inhibitor	Phase II
Liraglutide (Victoza/Saxenda)	GLP1R1 agonist	Phase II
Cenicriviroc (TBR-652)	Dual CCR2 and CCR5 antagonist	Phase II
BMS-986036	FGF21 agonist	Phase II
Tipelukast	LTD4 receptor antagonist	Phase II
ARI 3037 MO	Niacin analogue	Phase II
Volixibat (SHP626)	ASBT inhibitor	Phase II

ASBT, apical sodium bile acid cotransporter; CCR2, chemokine receptor agonist 2; CCR5, chemokine receptor agonist 5; FGF21, fibroblast growth factor 21; GLP1R, glucagon-like peptide 1 receptor; LTD4, leukotriene D4; LOXL2, lysyl oxidase homologue 2; MAPK5, mitogen-activated protein kinase 5.

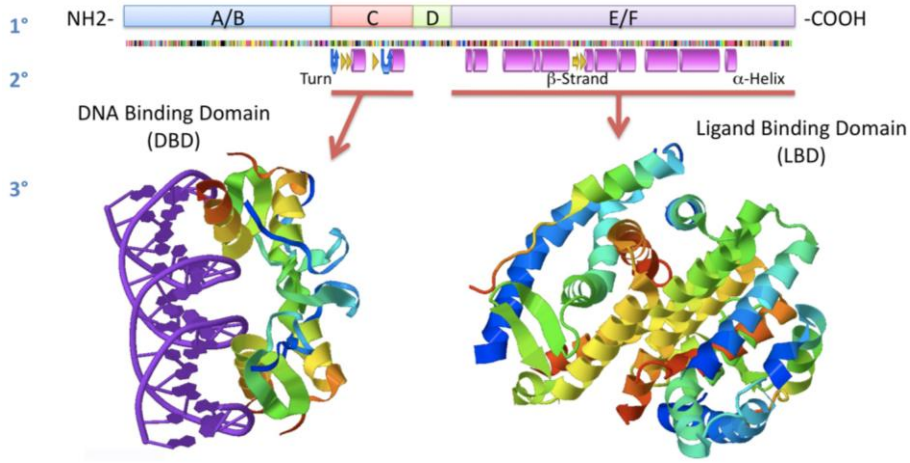

Figure 2. Primary, secondary and tertiary structure of nuclear receptors.

Most members of the nuclear receptor superfamily have a common domain structure consisting of an A/B domain in N terminus (termed activation function 1 (AF-1)), a central C domain (termed DNA-binding domain (DBD)), a D domain (termed hinge domain) and an E/F domain in C terminus (termed ligand-binding domain (LBD)). At the extreme C terminus, activation function 2 (AF-2) is located (Figure from Nuclear Receptor Resource (http://nrresource.org/)).

1.2. Nuclear receptor subfamily 1, group D, member 1 (NR1D1)

1.2.1. Expression and structure of NR1D1

Nuclear receptor subfamily 1, group D, member 1 (*Nr1d1*) was first identified to be located on the same region and transcribed from the reverse strand of the *thyroid receptor alpha* (*TRα*, also known as *ERBA*) gene, and hence it is called as *Rev-erbα* derived from 'reverse strand of *ERBA*' [Miyajima et al., 1989; Lazar et al., 1989, 1990].

NR1D1 is a ligand-regulated transcriptional factor that consists of an N-terminal activation function 1 (AF-1) region, a conserved DNA-binding domain (DBD), a linker region and a ligand-binding domain (LBD) [Kojetin et al., 2014]. The nuclear localization signals (NLSs) of Nr1d1 are specifically mapped within the DBD, and are responsible for subcellular distribution of Nr1d1. While most NLSs of nuclear receptors are located in the junction between the DBD and hinge, in the hinge, or in the LBD, the Nr1d1 has a specific and unusual NLS in the DBD [Chopin-Delannoy et al., 2003]. In addition, Nr1d1 lacks atypically the C-terminal activation function 2 (AF-2) domain, which recognizes transcriptional coactivators (Figure 3).

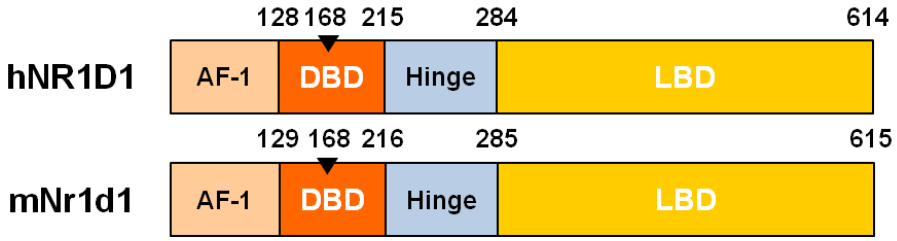

Figure 3. Structure of human NR1D1 and mouse Nr1d1.

Schematic presentation of amino sequences corresponding to human NR1D1 and mouse Nr1d1. Numbers above each receptor represent the amino acid position according to national center for biotechnology information, U.S. national library of medicine (NCBI) reference sequences. Flipped triangle (▼) means NLS, nuclear localization signal. AF-1, activation function 1 domain; DBD, DNA-binding domain; LBD, ligand-binding domain.

As a result, Nr1d1 binds to specific DNA response elements like Rev-erb direct repeats (RevDR2) and Rev-erb response element (RevRE) as monomers or homodimers, and recruits corepressors such as nuclear receptor corepressor (NCoR) and histone deacetylase 3 (HDAC3) to repress target gene transcription [Harding and Lazar, 1993, 1995; Adelmant et al., 1996; Yin and Lazar, 2005]. At this time, heme functions as a ligand for Nr1d1 via LBD, and stabilizes the interaction between Nr1d1 and NCoR [Yin et al., 2007; Raghuram et al., 2007] (Figure 4).

1.2.2. Roles and functions of Nr1d1 in pathophysiological processes

After its identification, the Nr1d1 has come into the spotlight with the circadian oscillator in a cell-autonomous manner [Preitner et al., 2002]. The robust circadian expressions of Nr1d1 in the mice were found in multiple tissues, and loss of Nr1d1 in mice resulted in disrupted circadian wheel-running behavior [Yamamoto et al., 2004; Cho et al., 2012]. Importantly, Nr1d1 was reported to serve in a negative feedback loop on the transcription of the core clock component Bmal1 to contribute circadian clockwork [Yin and Lazar, 2005]. Subsequent studies suggested that circadian clock genes such as Clock, and Npas2 were the transcriptional target genes of Nr1d1 [Crumbley et al., 2010; Crumbley and Burris, 2011]. Thus, Nr1d1 is an important component of the molecular clock and functions to regulate cellular circadian oscillations with multiple genes (Figure 5).

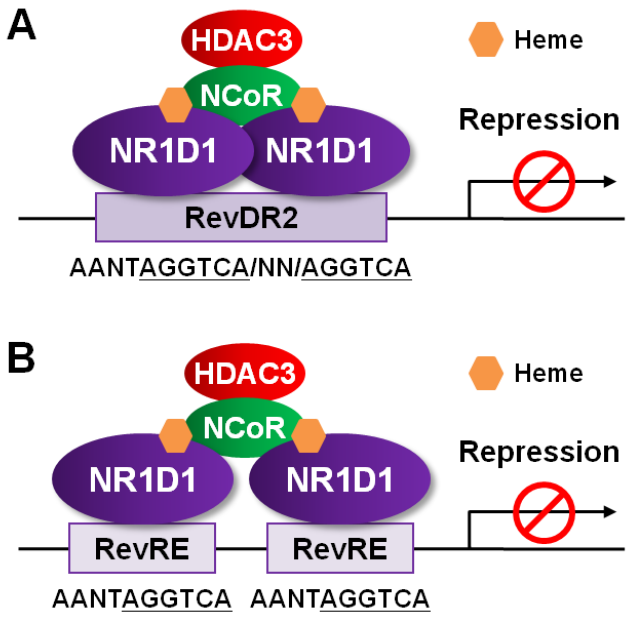

Figure 4. Modes of action of NR1D1.

(A) A heme-regulated Nr1d1 homodimer binds to a RevDR2 which two classical NR half sites AGGTCA flanked by an A/T-rich 5' sequence (AANT) are repeated and separated by 2bp (NN). The NCoR and HDAC3 complex is recruited by a heme-activated Nr1d1 homodimer. (B) Two Nr1d1 monomer bind to a RevRE consisting of an A/T-rich 5' sequence (AANT) and an AGGTCA core sequence. The NCoR and HDAC3 complex is also recruited by two heme-activated Nr1d1 monomers.

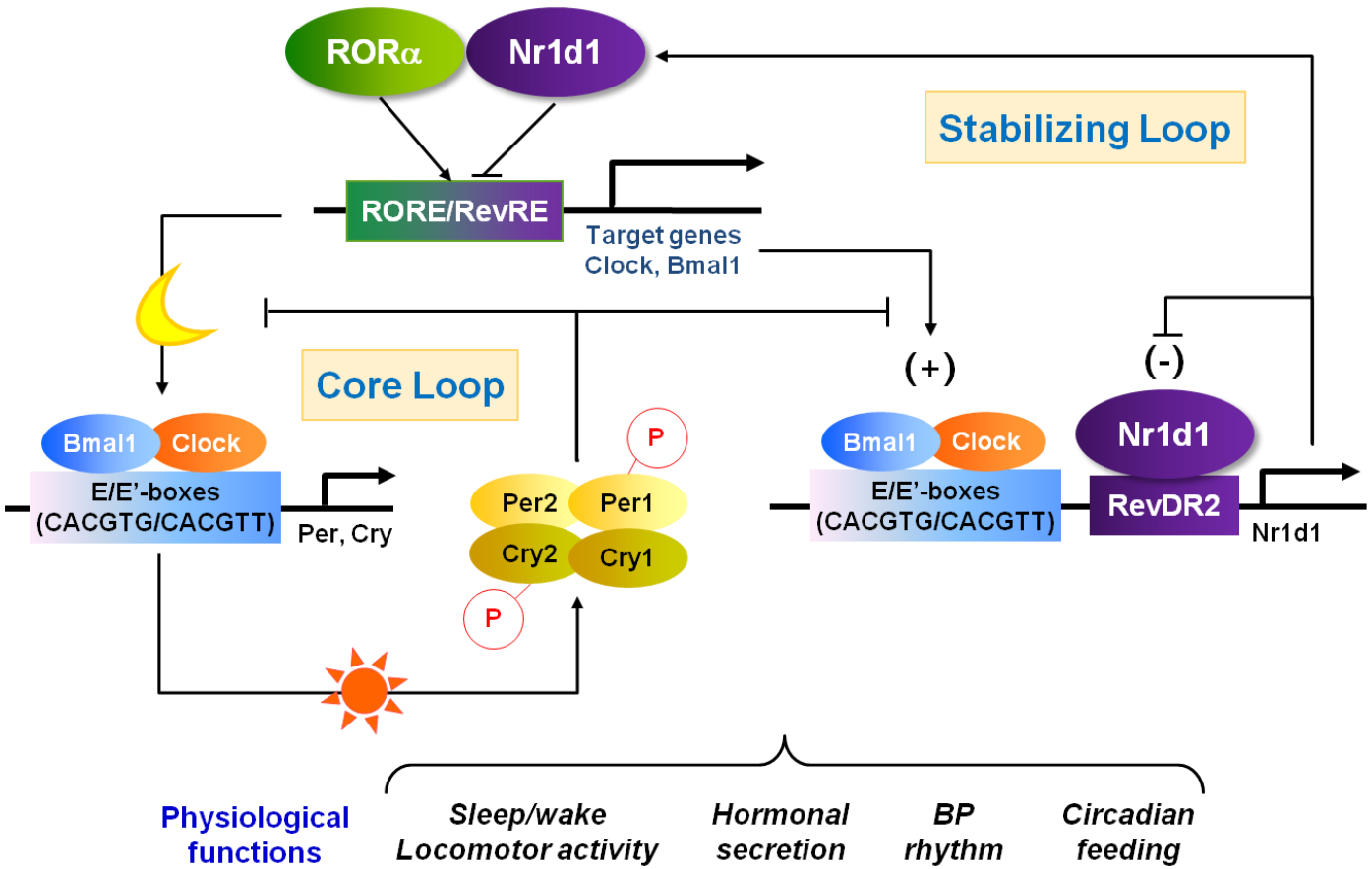
RORα
Nr1d1
Stabilizing Loop
RORE/RevRE
Target genes
Clock, Bmal1
Core Loop
(+)
(-)
Bmal1
Clock
E/E'-boxes
(CACGTG/CACGTT)
Per, Cry
P
Per2
Per1
Cry2
Cry1
P
Bmal1
Clock
E/E'-boxes
(CACGTG/CACGTT)
Nr1d1
RevDR2
Nr1d1
Physiological functions
Sleep/wake
Locomotor activity
Hormonal secretion
BP rhythm
Circadian feeding

Figure 5. Circadian clock loops.

The clock mechanism consists of a core (positive) and a stabilizing (negative) transcriptional feedback loop, which are intertwined via clock-protein-driven nuclear receptors and their interactions with Crys/Pers. Phosphorylation of the CRY and PER proteins regulate the negative feedback potential of these proteins on the Clock/Bmal1 complex. The transcription of Bmal1 is repressed by Nr1d1, controlling the amount of BMAL1 protein available for CLOCK binding. However, retinoic acid receptor-related orphan receptor alpha (RORα) exerts opposite effects to Nr1d1 on the Bmal1 promoter. Bmal1, brain and muscle ARNT-like 1; Clock, circadian locomotor output cycles protein kaput; Cry, cryptome; Per, period; RORE, ROR response elements.

Nr1d1 is abundantly expressed in a variety of tissues such as heart, brain, liver, kidney, skeletal muscle, lung, and adipose tissue [Miyajima et al., 1989; Forman et al., 1994]. Expression of Nr1d1 in the major metabolic tissues such as adipose tissue, skeletal muscle, and liver has been proved for its roles and function in regulation of metabolic processes. At first, studies of adipocytes demonstrated Nr1d1 is critical for white adipocytes differentiation with fat storage [Chawla et al., 1993; Fontaine et al., 2003; Wang and Lazar, 2008]. Recently, it was reported that Nr1d1 also regulates brown adipose tissue (BAT) formation and thermogenesis in BAT with energy expenditure [Gerhart-Hines et al., 2013; Nam et al., 2015]. In addition, roles of Nr1d1 in skeletal muscle biology have covered the modulation of myogenesis and mitochondrial biogenesis, impacting metabolic homeostasis [Downes et al., 1995; Pircher et al., 2005; Woldt et al., 2013]. Similar findings in the liver were reported that two key gluconeogenic genes, phosphoenolpyruvate carboxykinase (PEPCK) and glucose-6-phosphatase (G6Pase) were suppressed by Nr1d1, and hence, gluconeogenesis was inhibited, and glucose production was downregulated [Li et al., 2014; Fontaine et al., 2008].

Recent several data demonstrated that specific types of cells such as immune cells (e.g. macrophages and T cells), hepatic stellate cells, and endometrial stromal cells have high expression of the Nr1d1, which contributes inflammation, immunity, and tissue remodeling [Gibbs et al., 2012; Lam et al., 2013; Ma et al., 2013; Yu et al., 2013; Sato et al., 2014; Li et al., 2014; Isayama et al., 2015]. Interestingly, macrophages regulate inflammation via

circadian cytokines production, and their Nr1d1 was reported to control gene expression through the suppression of enhancer RNA transcription [Gibbs et al., 2012; Lam et al., 2013]. In this way, Nr1d1 provides a critical connection between the circadian clock and immune responses.

Besides those, Nr1d1 is a critical player in brain and behavior. The rhythmical expression of Nr1d1 in the suprachiasmatic nucleus (SCN) of the hypothalamus regulates circadian clock genes in the body, and it was confirmed by phase-advance in locomotor activity in genetically disrupted Nr1d1 mice [Cho et al., 2012]. Nr1d1 null mice exhibited the delay of postnatal development in the cerebellum, and the delay was overcome in adults [Raspé et al., 2002]. In addition, Nr1d1 null mice were reported to associate with behavioral abnormalities such as impaired memory formation, by displaying increased anxiety and depressive behaviors in the midbrain dopaminergic neurons [Duez et al., 2008].

Taken together, Nr1d1 acts in a variety of tissues to regulate circadian rhythms as well as metabolism, immune response, and behavioral activities (Figure 6). Given that NR1D1 is a coordinator of pathophysiology in human, NR1D1 should be a potential molecular player in the lipid metabolism and immune system in the liver. However, the precise involvement of NR1D1 in the pathogenesis of NAFLD has been questioned.

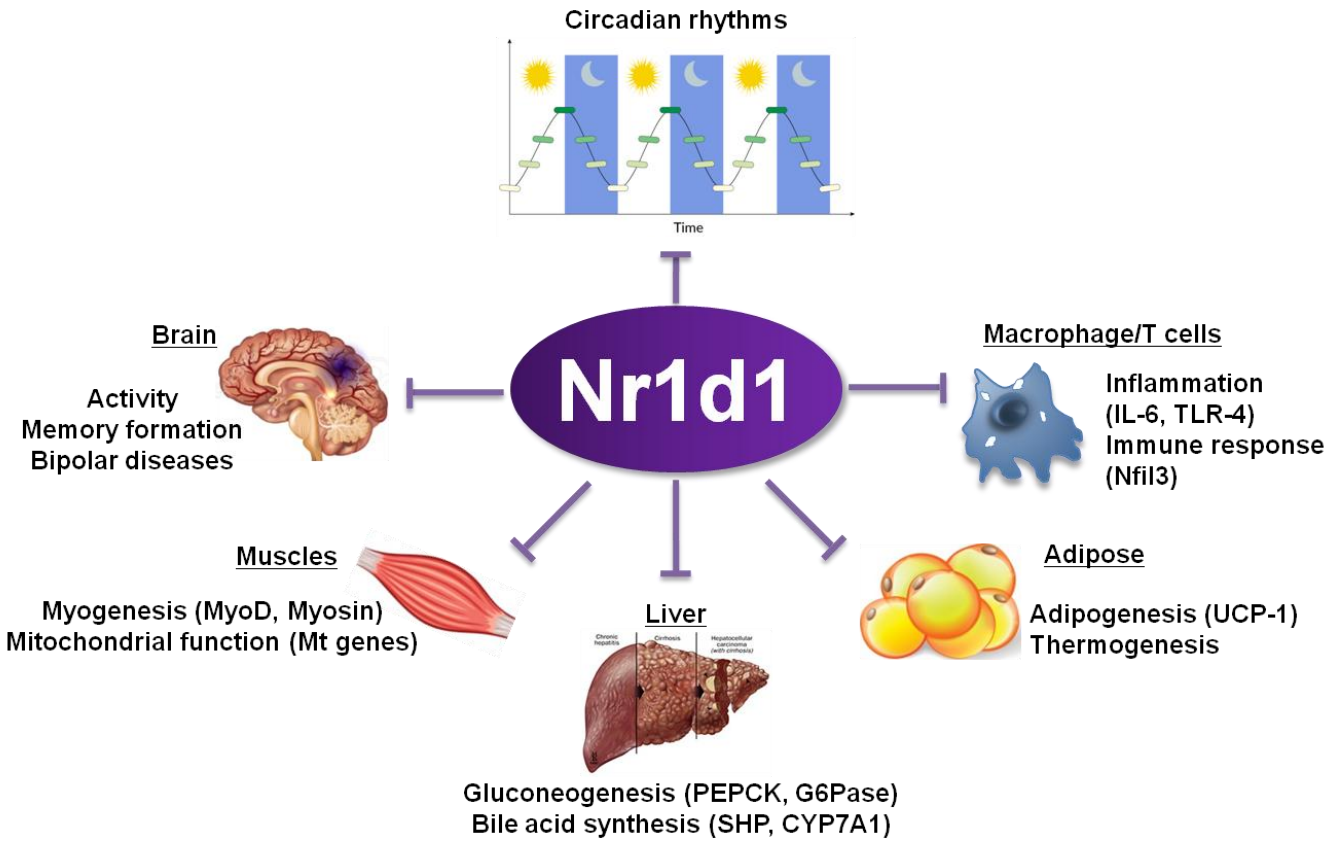

Figure 6. The roles of Nr1d1in various tissues and cells.

1.2.3. *In vitro* and *in vivo* models of Nr1d1 in NAFLD

The liver is a central organ for metabolic homeostasis, and Nr1d1 has been reported to regulate the circadian clock gene Bmal1 in the liver cells [Yin and Lazar, 2005; Preitner et al., 2002]. Studies within the past two decades have focused on the roles and functions of Nr1d1 in regulating bile acid metabolism and apo-lipoprotein CIII in the liver cells [Raspé et al., 2002; Duez et al., 2008; Le Martelot et al., 2009].

To more deeply understand the metabolic functions of Nr1d1 in the liver, several studies have been performed using genetic knockout or mutation approaches to disrupt the mouse *Nr1d1* gene. The Nr1d1 knockout ($Nr1d1^{-/-}$) mice, generated by systemically replacing target exons of *Nr1d1* with the gene encoding β-galactosidase, showed increased levels of hepatic triglycerides and altered hepatic lipid metabolism gene expression [Preitner et al., 2002; Chomez et al., 2000; Bugge et al., 2012; Delezie et al., 2012]. However, *Nr1d1* conditional knockout mice targeting exons 3 and 4 encoding the DNA-binding domain (DBD; Nr1d1 Δex3/4) exhibited no abnormality in hepatic steatosis [Zhang et al., 2015]. Meanwhile, Nr1d1 liver-specific promoter-driven transgenic mice (Tg-Nr1d1) showed that the transcriptions of the sterol regulatory element-binding protein (SREBP) 1 and 2 pathway genes were accumulated in the liver. These findings confirmed the hypothesis that the Nr1d1 controlled the lipogenesis and cholesterol metabolism [Le Martelot et al., 2009; Kornmann et al., 2007]. These discrepancies in the phenotypes of

these different Nr1d1 mutant strains have prevented complete understanding of the role of this gene in hepatic lipid metabolism.

The phenotypic analysis of these mice model has some problems. First, the definition of hepatic steatosis was not clinically precise. Still, most researchers have not measured and clinically analyzed the TGs in the livers [Preitner et al., 2002; Chomez et al., 2000; Bugge et al., 2012; Delezie et al., 2012; Zhang et al., 2015]. The definition of hepatic steatosis is the accumulation of cytoplasmic triglycerides in more than 5% of hepatocytes, or 55 mg/g liver tissue [Hardy et al., 2016]. The most data in several reports did not meet the clinical parameter of hepatic steatosis. Next, as NAFLD is a complex disease caused by various causes such as obesity and insulin resistance, the proper experimental models are required to copy the pathogenic condition of NAFLD. Most experiments were performed in normal condition, and were not in mimic condition for NAFLD. Thus, precise experimental conditions and clinical analysis should be introduced for the research of NAFLD.

1.3. Outline of this thesis

In this thesis, the aim of study was to clarify the role of NR1D1 in hepatic lipid metabolism and to understand the molecular pathogenesis of NAFLD. To remove the confusion from the discrepant hepatic phenotypes of the animal models of Nr1d1, the whole-body *Nr1d1* Δex3/4 mice, in which deletion of *Nr1d1* exons 3 and 4 for a functional disruption was introduced, were generated by crossing *Nr1d1* floxed mice with transgenic Zp3-Cre deleter mice. Because NAFLD is caused by a variety of metabolic syndromes with heterogeneous pathogenesis, mouse models based on the disruption of single genes frequently fail to recapitulate its pathophysiology [Day, 2002]. Therefore, dietary challenges such as the administration of a high-fat diet (HFD) are often indispensable for studying mouse models of NAFLD [Hardy et al., 2016]. The Nr1d1 Δex3/4 mice were treated by HFD, and the metabolic phenotypes that responded to these stimuli were observed. In addition, to understand the potential molecular mechanism, the differential gene expression was profiled using microarray, and upstream factors and gene coexpression networks were predicted. In addition, the liver-specific Nr1d1 LΔex3/4 mice were generated, and the phenotypic observation of the whole-body Δex3/4 mice was compared and analyzed. The advantages of experimental NAFLD models and the interaction effect of gene-diet are discussed. The unique strengths of this mice model are addressed as well.

2. Materials and methods

2.1. Animal studies

2.1.1. The generation of *Nr1d1* Δexon3/4 mice

Frozen embryos obtained from the conditional knockout mice *Nr1d1*$^{tm1Ics/+}$ (PHENOMIN-Institut Clinique de la Souris, Illkirch Cedex, France) with flox/flox sites targeting exons 3 and 4 of the mouse *Nr1d1* were thawed and transferred to pseudopregnant female C57BL/6J mice at the laboratory of the animal resources center of Korea Research Institute of Bioscience & Biotechnology (Daejeon, Republic of Korea). The Nr1d1 Δexon3/4 mice were generated by crossing with *Nr1d1*$^{flox/+}$ mice and Zp3-Cre or Alb-Cre transgenic mice as described previously [Jeon et al., 2011; Lee et al., 2016]. The mice were genotyped by polymerase chain reaction (PCR) amplification.

2.1.2. The treatment of HFD in Nr1d1 Δexon3/4 mice

Seven-week-old male mice were fed a low-fat diet (LFD; D12450Bi, Research Diets, New Brunswick, NJ, USA) or a HFD (D12492, Research Diets) for 12 weeks. Body weights were recorded every other week, and at the end of observation period liver weight were measured. After 10 weeks diets, metabolic assessment using the Comprehensive Lab Animal Monitoring System (Oxymax/CLAMS, Columbus Instruments, Colombus, OH) was performed with a method of indirect calorimetry. Following an initial 4 hour

acclimatization period, oxygen consumption and carbon dioxide production in mice were monitored every 30 minute for 40 hours to complete a 12 hour night (active)/12 hour day (inactive)/12 hour night (active) cycle. These measurements were then used to calculate the respiratory exchange ratio (RER, RER = VCO2/VO2). Metabolic rates were normalized to total body, and results were averaged over 0.5 hour intervals in order to smooth out the substantial point-to-point variation. All animal procedures were approved by the Institutional Animal Care and Use Committee of Seoul National University and the National Cancer Center.

2.1.3. Histology and serum/liver biochemistry analysis

Paraffin wax-embedded liver tissues were sectioned and stained with hematoxylin and eosin (H&E), and Oil-Red O (ORO) staining of frozen liver sections was performed as described [Lee et al., 2008]. Hepatic triglyceride (TG) content was determined by ethanolic potassium hydroxide saponification followed by an assay for glycerol as described [Norris et al., 2003]. The serum levels of alanine transaminase (ALT) and aspartate aminotransferase (AST) were determined by standard clinical chemistry assays on an Automated Clinical Chemistry Analyzer (Fuji DRI-Chem 3500s, FUJIFILM Corporation, Tokyo, Japan).

2.2. Cells and cell culture

2.2.1. NIH3T3 cells culture

The mouse embryo fibroblast NIH3T3 cell line (CRL-1658™, American Type Culture Collection, Manassas, VA, USA) was grown in Dulbecco's modified Eagle's medium (GE Healthcare, Logan, UT, USA) supplemented with 10% fetal bovine serum (GE Healthcare) and 1% penicillin/streptomycin (Life Technologies, Grand Island, NY, USA).

2.2.2. MEF preparation and culture

Mouse embryonic fibroblast (MEF) cells were prepared at embryonic day 13.5 from timed mating between *Nr1d1*$^{+/\Delta}$ mice, and the genotypes were determined by PCR as described [Jeon et al., 2011]. MEFs were used at passages two to five, and were maintained in Dulbecco's modified Eagle's medium containing 10% fetal bovine serum, 2 mM glutamine, and 0.1 mM 2β-mercaptoethanol. Cells were cultured in humidified 5% CO2/95% air at 37 ℃.

2.3. Transient transfection, and reporter gene analysis

2.3.1. Transient transfection

Coding sequences of the wild-type (WT) *Nr1d1* and the *Nr1d1* Δex3/4 genes were prepared from corresponding mouse livers and cloned into pCMV-Myc or pEGFP-C3 vectors. Transient transfection of these plasmids into NIH3T3 cells was performed using Polyfect (Qiagen, Valencia, CA, USA).

2.3.2. Reporter gene analysis

The *Bmal1* (−816 to +99) promoter-luciferase (Luc) and *Nr1d1* (6.6kb) promoter–Luc constructs were generously provided by Dr. Kyungjin Kim (Daegu Gyeongbuk Institute of Science and Technology, Daegu, Republic of Korea) and Dr. Urs Albrecht (University of Fribourg, Fribourg, Switzerland), respectively [Yu et al., 2002; Schmutz et al., 2010]. Reporter gene assays were performed as described [Lee et al., 2012].

2.4. Quantitative reverse transcription PCR (RT-qPCR)

Total RNA was prepared and reverse transcribed to cDNA using First Strand cDNA Synthesis kits (Roche Applied Science, Mannheim, Germany). PCR reactions were performed using a Power SYBR Green PCR Master Mix

(Thermo Fisher Scientific Inc., Waltham, MA, USA) on a StepOnePlus Real-Time PCR System (Applied Biosystems, Foster City, CA, USA). The baseline cycles and threshold (CT) were autocalculated in PCR baseline-subtracted mode using the system's software. Gene expression levels were normalized against that of *18S rRNA* and determined relative to controls using the $2^{-\Delta\Delta CT}$ method [Livak et al., 2001]. The RT-qPCR primer sequences were in Table 2.

2.5. Western blotting, fluorescence microscopy, and chromatin immunoprecipitation (ChIP) assay

2.5.1. Western blotting

Whole cell lysates, nuclear, and cytosolic fractionations were prepared as described [Yoo et al., 2008]. Western blotting was performed using specific antibodies against Actin, Myc, YY-1 (Santa Cruz Biotechnology, Inc., Dallas, TX, USA) and α-tubulin (Merck Millipore, Darmstadt, Germany).

2.5.2. Fluorescence microscopy

To localize the expression of proteins, immunofluorescence staining was performed. Nr1d1 WT and Δex3/4 MEF cells were stained with specific anti-Nr1d1 antibody (1:100) (Proteintech Group, Inc., USA) or control IgG (1:100) (Santa Cruz Biotechnology). DAPI was used to stain the nuclei.

Table 2. Gene specific primers used in RT-qPCR

Gene	Forward primer	Reverse primer
Nr1d1 exon 2	5′–TAC ATT GGC TCT AGT GGC TCC–3′	5′–CAG TAG GTG ATG GTG GGA AGT A–3′
Nr1d1 exons 3/4	5′–TGG CAT GGT GCT ACT GTG TAA GG–3′	5′–ATA TTCT GTT GGA TGC TCC GGC G–3′
Nr1d1 exon 5	5′–GCT CAG CGT CAT AAT GAA GCG–3′	5′–GGG CCG AAT ATA CGT GGG T–3′
Nr1d1 exons 6/7	5′– GAC CTT TCT CAG CAC GAC CAG–3′	5′– GCG GCT CAG GAA CAT CAC TGT–3′
Nr1d1 exons 8	5′–TAT TCC AAG ATG AGC CTC TGG C–3′	5′– GGT GGA GAG AGC AAG AGT GGT–3′
Nr1d1 exons 2/5	5′–TGT CCC CCA GCA AGG GCA CAA–3′	5′–TGC TTC TCT CTC TTG GGG ATG C–3′
Thrsp	5′–GAA ACG GAG GAG GCC GAA GAA G–3′	5′–GTT GAT GCA CCT CGG GGT CTT C–3′
18S rRNA	5′–GTA ACC CGT TGA ACC CCA TT–3′	5′–CCA TCC AAT CGG TAG TAG CG–3′

To examine the intracellular localizations of Nr1d1, pEGFP-Nr1d1 WT or pEGFP-Nr1d1 Δex3/4 were transiently expressed in NIH3T3 cells and fluorescence microscopy was performed.

2.5.3. Chromatin immunoprecipitation (ChIP) assay

ChIP assay was performed using an anti-Nr1d1 antibody (Proteintech Group, Inc., Rosemont, IL, USA) or a control IgG antibody (Santa Cruz Biotechnology) as described [Lee et al., 2012]. Specific primers for the sequences of Nr1d1 binding site on the *Bmal1* promoter and the *Nr1d1* promoter were: for the *Bmal1* promoter, sense, 5′−AAT TGG TTT GGG TTG TCC GCC AAG–3′, and antisense, 5′–TAA ACA GGC ACC TCC GTC CC–3′; for the *Nr1d1* promoter, sense, 5′–ACA CGC CAC CCT GAC TCT TCA–3′, and antisense, 5′–CTT TTG CCC GAG CCT TTC–3′.

2.6. Microarray experiments and data analysis

2.6.1. Microarray experiments

RNA samples were preprocessed using the GeneChip WT PLUS Reagent Kit (Affymetrix, Santa Clara, CA, USA). Biotin-labeled DNA was hybridized to a GeneChip Mouse Gene 2.0 ST Array (Affymetrix). Subsequently, hybridized arrays were followed by washing and staining on a GeneChip Fluidics Station

450 (Affymetrix) and scanned on a GCS3000 Scanner (Affymetrix). Data processing was performed according to the GeneChip Command Console software (Affymetrix).

2.6.2. Data analysis

Differentially expressed gene analysis was performed with data normalized according to the robust multi-average method. Statistical significance of the expression data was determined using fold changes and two-way analysis of variance (ANOVA) in which the null hypothesis was that no significant difference existed among two groups for each factor (diet and genotype). The false discovery rate (FDR) was controlled for by adjusting P-values using the Benjamini–Hochberg algorithm [Lee et al., 2008].

Gene enrichment and functional annotation analysis for significant probe lists was performed using ToppGene Suite (https://toppgene.cchmc.org/) with a hypergeometric probability mass function [Chen et al., 2009]. Transcription factor binding site (TFBS) enrichment was analyzed using single site analysis in oPOSSUM 3.0 (http://opossum.cisreg.ca/oPOSSUM3/), a web-based system that can detect overrepresented conserved TFBSs in sets of genes or sequences [Kwon et al., 2012]. Coexpressing gene networks were predicted using the Cytoscape plug-in GeneMANIA in all interaction networks for Mus musculus, the top 20 related genes were found using an automatic weighting method [Warde-Farley et al., 2010].

2.7. Statistical analysis

Except for the microarray experiments, all data are expressed as the mean ± standard error of mean (SEM). Unpaired Student's t tests or Mann-Whitney nonparametric U tests or two-way ANOVA tests were used to detect differences between means in data sets containing two groups. Statistical significance was set at $P < 0.05$. Graphs were prepared and data analyzed using GraphPad Prism version 5 (GraphPad Software, La Jolla, CA, USA).

3. Results

3.1. Generation of whole-body *Nr1d1* Δex3/4 mice

3.1.1. The strategy of floxed *Nr1d1* and generation of whole-body *Nr1d1* Δex3/4 mice

To functionally disrupt the DBD in the *Nr1d1* gene, the Cre/loxP recombination system to target *Nr1d1* exons 3 and 4 was used (Figure 7). Exons 3 and 4 of the *Nr1d1* gene encode the DBD region. Mice with *Nr1d1* floxed allele were crossed with transgenic Zp3-Cre deleter mice, expressing a Cre recombinase in the oocytes, and to generate the *Nr1d1* exons 3 and 4-deleted allele mice as germline knockout mice [Lewandoski et al., 1997; Jeon et al., 2011]. In this mouse system, removal of these exons should have resulted in a frame shift in the coding region after splicing from exon 2 to exon 5. The targeting vector was designed to introduce a loxP site in intron 2 and a loxP in intron 4. Therefore, the resultant mutant mice were named *Nr1d1* exons 3 and 4 deleted (Nr1d1 Δex3/4) mice.

After a fragment of amino acids 125-203 was deleted, the subsequent restoration of the reading frame substituted a threonine molecule between exons 2 and 5 (Figure 8A). Because of no in-frame stop codon in the downstream exons, the predicted translated protein was expected to be composed of 537 amino acids from Nr1d1 and one amino acid from the frame shift in exons 2 and 5 and should lack the DBD of Nr1d1. As a result, the *Nr1d1* Δex3/4-encoded mutant protein was produced, and the molecular

weight of the *Nr1d1* Δex3/4-encoded mutant protein obtained from MEF cells was approximately 58 kDa, smaller than approximately 67 kDa of the Nr1d1 WT protein obtained from MEF cells (Figure 8B). Strikingly, the protein expression level of the Nr1d1 Δex3/4 was higher than that of the WT in MEF cells.

Next, it was verified whether the exons 3 and 4 of *Nr1d1* were deleted by comparing the mRNA levels between other exon regions (Figure 9). RNA was extracted from livers and analyzed by RT-qPCR using different primers sets. First of all, as expected, the *Nr1d1* Δex3/4 transcripts lacked in the exons 3 and 4 (3/4), a deleted region. On the other hand, the mRNA levels of the non-deleted regions were dramatically increased in the in the Nr1d1 Δex3/4 mice compared to the Nr1d1 WT mice. In addition, after the deletion of exons 3 and 4 in *Nr1d1*, mRNA was present in the liver. The splicing had occurred between exons 2 and 5 (2/5) in the Nr1d1 Δex3/4 mice. Indeed, the different lengthed RT-qPCR products were made from each other: 304 base pairs for the *Nr1d1* WT and 70 base pairs for the *Nr1d1* Δex3/4, respectively. Similar to the protein expression, the mRNA expression levels of the *Nr1d1* Δex3/4 in the non-deleted regions were increased than that of the WT gene in mouse livers.

Therefore, expression of proteins as well as RT-qPCR data confirmed deletion of the *Nr1d1* exons 3 and 4, and showed that a splicing had occurred and the Nr1d1 Δex3/4 mutant protein was produced in these mice.

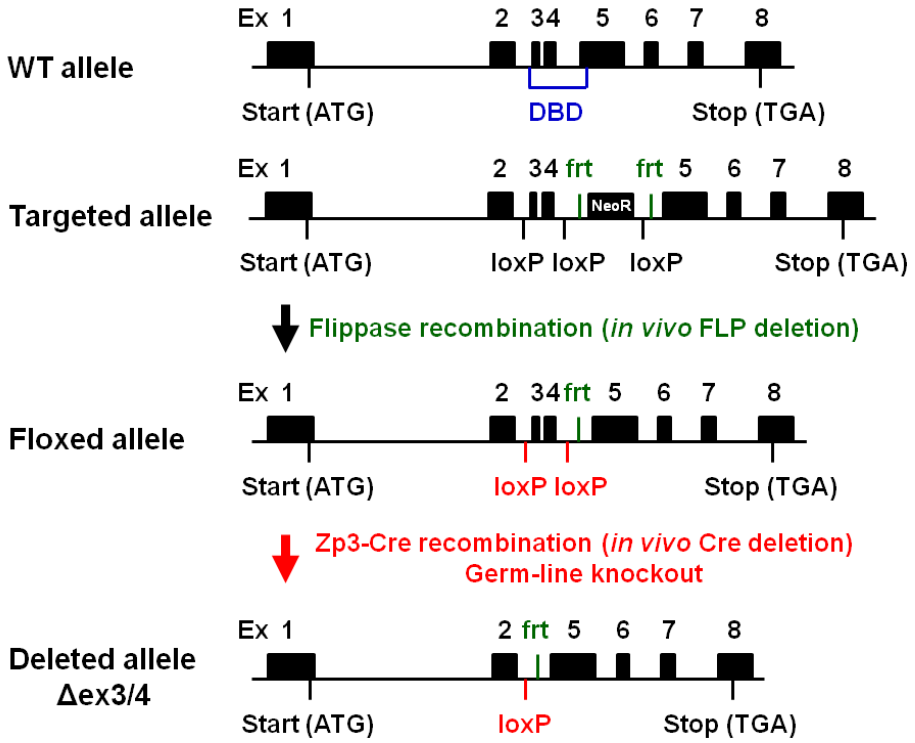

Figure 7. The strategy of the whole-body Nr1d1 Δex3/4 mice.

The *Nr1d1*^{tm1Ics} mouse is a conditional knockout mouse system targeting exons 3 and 4 encoding DNA binding domain (DBD). Floxed allele mice were crossed with Zp3-Cre mice, and deleted allele mice were generated. Numbers above each allele represent the exon position. Ex, exon; frt, flippase recognition target; FLP, flippase.

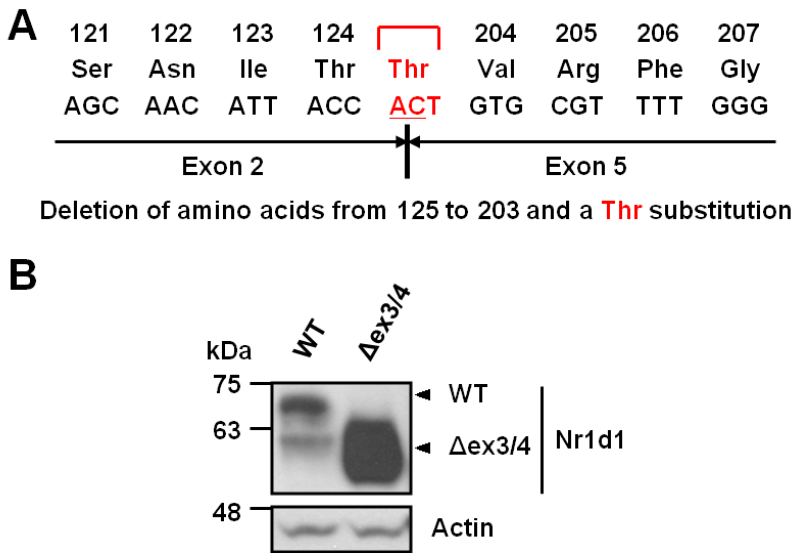

Figure 8. Targeted disruption of the mouse *Nr1d1* exons 3 and 4 results in a DBD-deleted mutant mouse.

(A) A splicing between exons 2 and 5 in the *Nr1d1* Δex3/4 resulted in generation of an in-frame codon (ACT) for a threonine (Thr). (B) Whole cell lysates obtained from the WT and the Nr1d1 Δex3/4 MEF cells were analyzed by western blotting with the specific antibody for Nr1d1 and Actin.

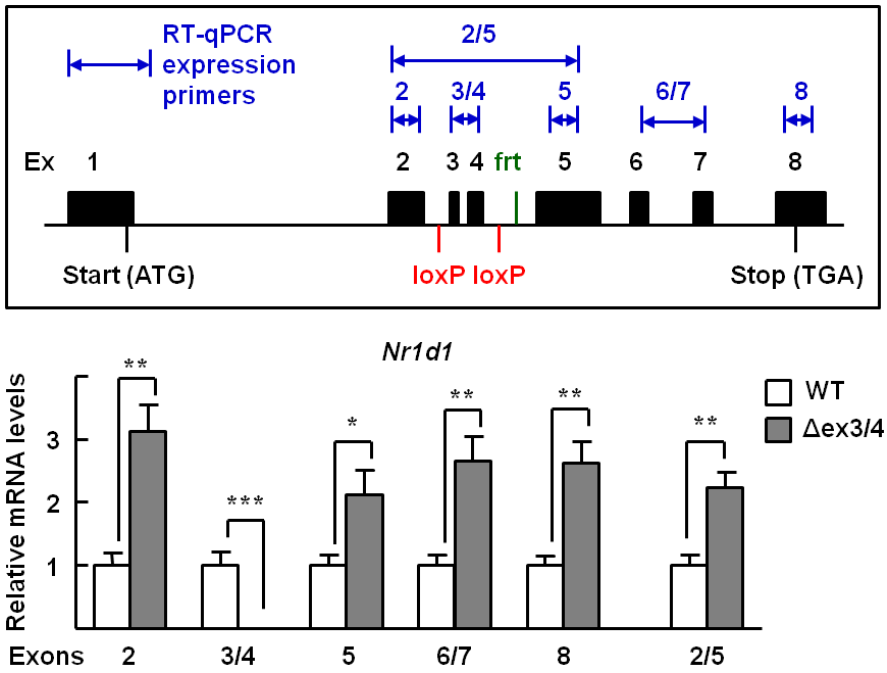

Figure 9. Hepatic mRNA expression of the WT and the Nr1d1 Δex3/4 mice.

Hepatic mRNA expression levels of the WT and the Nr1d1 Δex3/4 mice were measured by RT-qPCR using different sets of primers as indicated in the above graphic. Values represent mean ± SEM (n=6-8). * $P < 0.05$, ** $P < 0.01$ and *** $P < 0.001$.

3.1.2. The Nr1d1 Δex3/4 mutant protein is located in both the nuclei and cytoplasm of the cells.

Although the hepatic expression in the Nr1d1 Δex3/4 mice was defective, the Nr1d1 Δex3/4 protein expression was excessive in the cells. It is required to verify the basic characteristics of the mutant protein. Hence, it was first examined where the Nr1d1 Δex3/4 protein was expressed in the cells. Nr1d1 is a nuclear protein as named, and it has been reported that Nr1d1 has a NLS in the DBD region, which disrupted in the Nr1d1 Δex3/4 mice [Chopin-Delannoy et al., 2003]. Thus, the subcellular localization of the Nr1d1 Δex3/4 protein is important for understanding nuclear function.

To define the subcellular distribution of the Nr1d1 Δex3/4 protein precisely, immunofluorescence microscopy was used. The Nr1d1 Δex3/4 protein was widely localized in the nuclei and cytoplasm of the Nr1d1 Δex3/4 MEF cells, whereas the Nr1d1 WT protein was mainly localized in the nuclei of the WT MEF cells (Figure 10). The Nr1d1 Δex3/4 MEF cells present more strong signals than the WT MEF cells. It is consistent with the data that the Nr1d1 Δex3/4 protein was intensively expressed in the MEF cells (Figure 8B).

To ensure the localization of the Nr1d1 Δex3/4 protein *in vitro*, the expression vectors for the *Nr1d1* Δex3/4 gene were constructed by PCR amplification using the hepatic cDNA as a template. By fluorescence microscopy, the green fluorescent protein (GFP)-fused Nr1d1 Δex3/4 protein was detected in both

the nuclei and cytoplasm of NIH3T3 cells, and the GFP-fused Nr1d1 WT protein was present in the nuclei of NIH3T3 cells (Figure 11). Interestingly, the fluorescence microscopy revealed that the GFP-fused Nr1d1 Δex3/4 protein was accumulated in cytoplasm, indicating the high expression levels of the Nr1d1 Δex3/4 protein.

To further analyze the subcellular distribution of the Nr1d1 Δex3/4 protein, a murine cell line, NIH3T3 cells and transiently transfected Myc-*Nr1*d1 WT or Δex3/4 sequences. The molecular weight of the transiently expressed Nr1d1 Δex3/4 protein was the same as for that isolated from the mice liver. The level of Nr1d1 Δex3/4 protein was much higher than that of the WT gene although the same amount of plasmid had been transfected, consistent with *in vivo* observations in Figure 8B. Subcellular fractionation revealed that the Nr1d1 Δex3/4 protein was located in both the nuclei and cytoplasm, whereas the WT protein was located mainly in nuclei. In addition, as already found for the Nr1d1 Δex3/4 protein, significant accumulation of the proteins was found in the cytoplasm than in the nuclei (Figure 12).

Based on these observations, the Nr1d1 Δex3/4 protein was found in both the nuclei and cytoplasm, and was intensively accumulated in the cytoplasmic distribution.

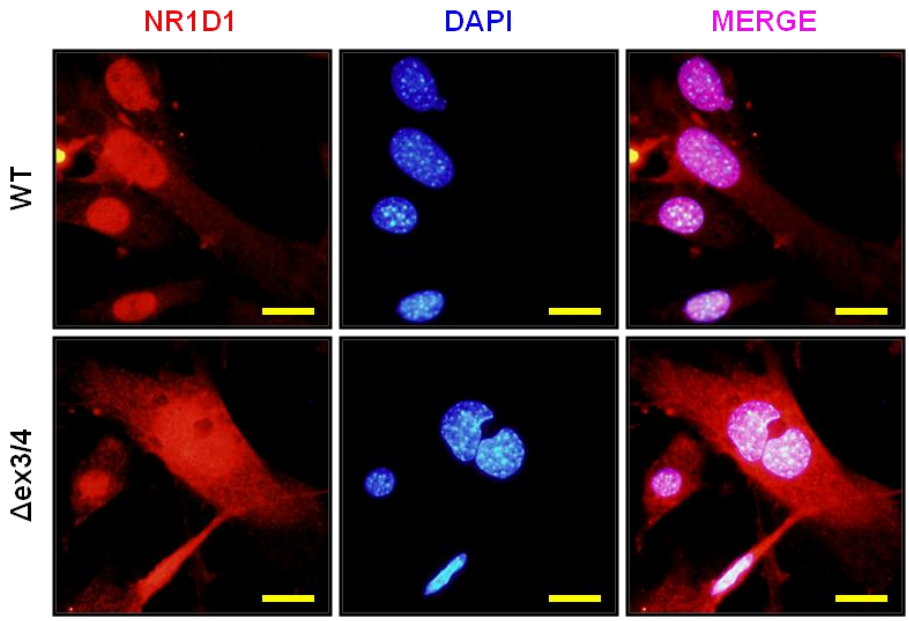

Figure 10. Localization of the Nr1d1 proteins in the WT and Nr1d1 Δex3/4 MEF cells.

The WT and Nr1d1 Δex3/4 MEF cells were fixed and stained for the Nr1d1 using the specific anti-Nr1d1 antibody (red). DAPI was used to counterstain the nuclei (blue). Pink displays colocalization of the Nr1d1 proteins with nuclei. Representative images are shown (600X magnification). Scale bar: 20 μm.

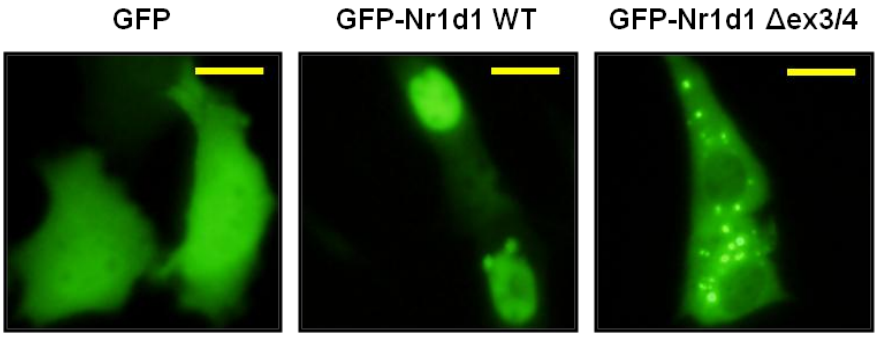

Figure 11. Localization of the Nr1d1 WT and Nr1d1 Δex3/4 proteins in the transiently transfected NIH3T3 cells.

NIH3T3 cells were transfected with the pEGFP-Nr1d1 WT or pEGFP-Nr1d1 Δex3/4, and then cellular localizations of the GFP-fused proteins were examined by fluorescence microscopy. Representative images are shown (400X magnification). Scale bar: 25 μm.

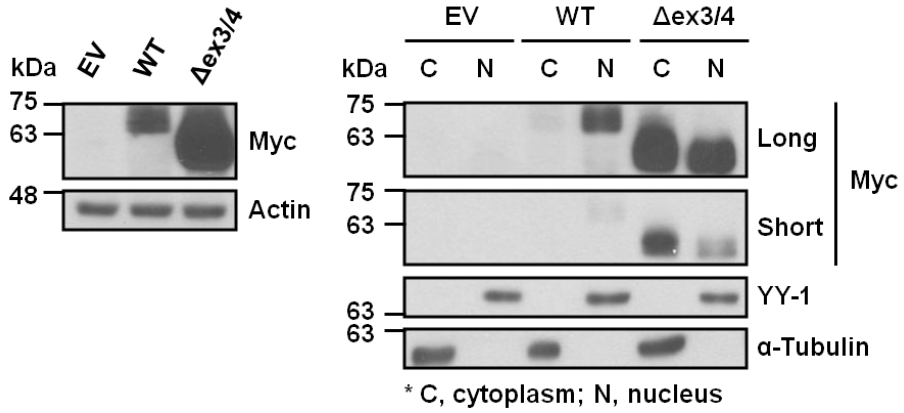

Figure 12. Intracellular distribution and cytoplasmic accumulation of the Nr1d1 Δex3/4 protein in NIH3T3 cells.

NIH3T3 cells were transfected with pCMV-Myc-Nr1d1 WT, pCMV-Myc-Nr1d1 Δex3/4, or empty vector (EV). After 24 h of transfection, whole cell lysates were tested for the Nr1d1 expression by western blotting (left). Or cells were fractionated into nucleus (N) and cytoplasm (C), and each fraction was analyzed by western blotting (right). Expressions of YY-1 and α-tubulin were analyzed as a marker for the nucleus and the cytoplasm.

3.1.3. The Nr1d1 Δex3/4 protein does not have transcriptional activity.

Next, it was tested whether the transcriptional function of the Nr1d1 Δex3/4 protein takes action performing reporter gene assays using the luciferase reporter-encoding promoters of *Bmal1* or *Nr1d1* which are well-known downstream genes [Yu et al., 2002; Schmutz et al., 2010]. The *Bmal1* promoter contains two Rev-erb response elements (RevREs), to which a Nr1d1 binds independently as monomers, whereas the *Nr1d1* promoter contains the Rev-erb direct repeat 2 (RevDR2), on which two Nr1d1 bind as a homodimer [Everett et al., 2014]. The Nr1d1 WT reduced the transcriptional activities from both reporter genes according to the expression levels of the construct, but the Nr1d1 Δex3/4 did not repress the transcription of both reporter genes (Figure 13).

A structural defect in the nuclear receptors has the dominant negative effects to interrupt the wild type receptors' transcriptional abilities [Achermann and Jameson, 2003]. Since the Nr1d1 Δex3/4 loss only DBD and retain the other domains such as AF-1 and LBD, it is required to evaluate the dominant negative effect of the Nr1d1 Δex3/4 mutant. Cotransfection of 1:1 equal and 10:1 excess of the Nr1d1 WT or the Nr1d1 Δex3/4 along with the Nr1d1 WT had no effect on wild type transcriptional activity so that the measured luciferase activity remained near the activity repressed by the Nr1d1 WT (Figure 14). Thus, the deletion of the DBD region in Nr1d1 has no dominant

negative effect.

In addition, it was confirmed by ChIP assays in the MEF cells that the Nr1d1 Δex3/4 protein did not bind to the site-specific DNA regions of *Bmal1* and *Nr1d1* promoters containing either RevREs or RevDR2 in contrast to the Nr1d1 WT protein (Figure 15). Although the Nr1d1 Δex3/4 is present in nuclei, it did not exhibit the site-specific DNA binding activity.

Together, these results demonstrated that the Nr1d1 Δex3/4 protein lost the transcriptional activity because of the lack of DNA binding, and did not render the Nr1d1 WT protein unable to bind to the Nr1d1 response elements.

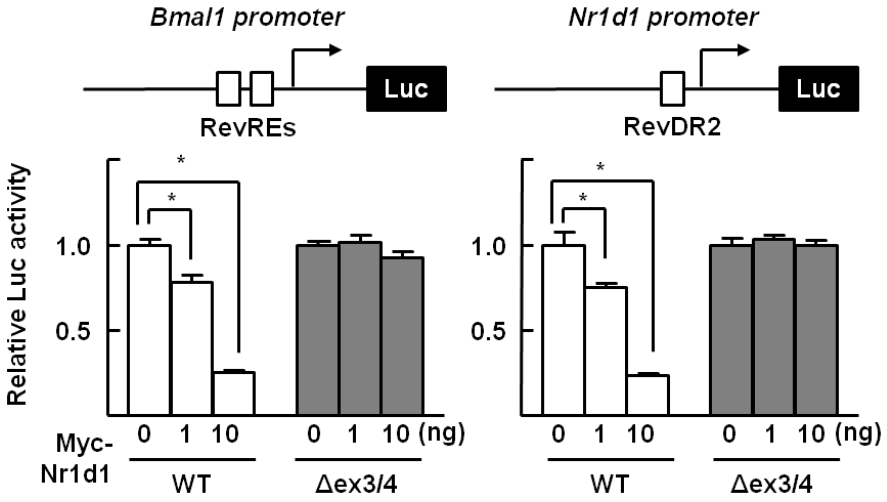

Figure 13. The Nr1d1 Δex3/4 mutant protein does not have transcriptional activity.

Transcriptional activities of the WT and the Nr1d1 Δex3/4 were determined by reporter gene assays using the *Bmal1* promoter-Luciferase (Luc) and the *Nr1d1* promoter-Luc in NIH3T3 cells. The reporter activity values were normalized by β-galactosidase activity values. Values represent mean ± SEM (n=4), * $P < 0.05$.

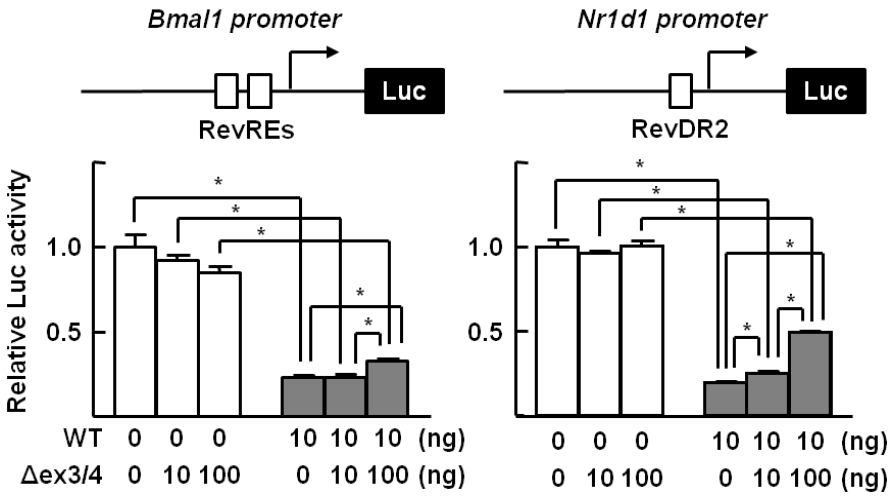

Figure 14. The Nr1d1 Δex3/4 has no dominant negative effect on the site-specific DNA containing RevREs and RevDR2.

Transcriptional activities of the WT and the Nr1d1 Δex3/4 were determined by reporter gene assays using the *Bmal1* promoter-Luc and the *Nr1d1* promoter-Luc in NIH3T3 cells. The reporter activity values were normalized by β-galactosidase activity values. Values represent mean ± SEM (n=4), * $P < 0.05$.

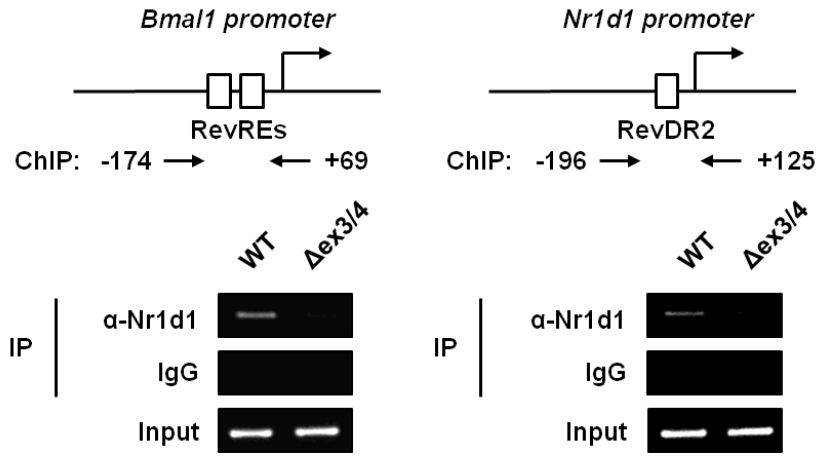

Figure 15. The Nr1d1 Δex3/4 does not have the DNA binding activity to the site-specific DNA.

The levels of DNA binding of the WT and the Nr1d1 Δex3/4 protein in MEF cells were analyzed by ChIP assays using the specific antibody for Nr1d1 and the primer sets as indicated.

3.2. Enhanced hepatic steatosis in the Nr1d1 Δex3/4 mice after HFD feeding

3.2.1. The Nr1d1 Δex3/4 mice are more prone to HFD-induced obesity

To elucidate the function of the *Nr1d1* gene in the pathogenesis of NAFLD, the 7-week-old male WT and Nr1d1 Δex3/4 mice were fed with LFD or HFD for 12 weeks. The 7-week-old Nr1d1 Δex3/4 mice exhibited no difference in body weights compared to the Nr1d1 WT mice. At the end of the HFD feeding of 10 weeks, the WT mice fed HFD were significantly heavier than both the WT and the Nr1d1 Δex3/4 mice maintained on LFD. Interestingly, the body weight increase confirmed that the Nr1d1 Δex3/4 mice highly responded the HFD-induced obesity compared to the Nr1d1 WT mice, and it indicated the susceptibility of the observed HFD-induced obesity was caused by the genotype (Figure 16).

In addition, to test whether the utilization of whole body fuels is modified in the Nr1d1 Δex3/4 mice, the energy metabolism *in vivo* was assessed by indirect calorimetry after 10 weeks diets. The RER (the ratio of carbon dioxide production to the oxygen consumption) indicates the types of fuels being oxidized for energy. A high RER (closer to 1.0) means that carbohydrates are being predominantly used, whereas a low RER (closer to 0.7) suggests that lipid is the predominant fuel source [Porter and Cohen, 1996; Paglialunga and Dehn, 2016]. The RERs on average were

approximately 0.9 in LFD-fed WT mice and 0.85 in LFD-fed Nr1d1 Δex3/4 mice, and there was a significant difference between WT and Nr1d1 Δex3/4 mice. On the other hand, both the HFD-fed WT and the Nr1d1 Δex3/4 mice had the similar RERs of approximately 0.7, indicating fat is the predominant fuel source (Figure 17).

These data demonstrated that the body weights of the Nr1d1 Δex3/4 mice had susceptibility to HFD-induced obesity. The Nr1d1 Δex3/4 mice were increased basal lipid utilization compared to the Nr1d1 WT mice with LFD feeding, and displayed a fat-prone metabolism with HFD as well as the Nr1d1 WT mice. Thus, the Nr1d1 is obligatory for a HFD-induced phenotype.

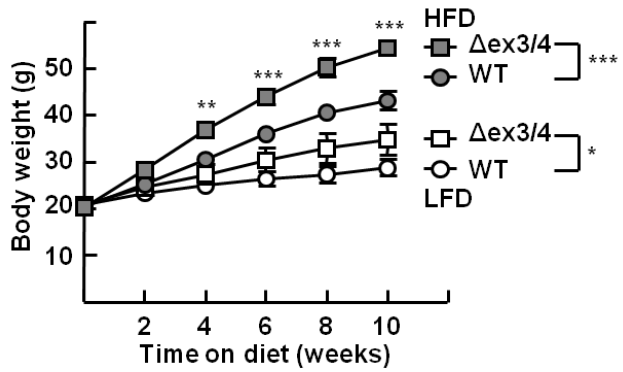

Figure 16. The body weights of Nr1d1 Δex3/4 mice are susceptible to the HFD.

Body weights were measured every other weeks in the WT and the Nr1d1 Δex3/4 mice fed a LFD or a HFD for 10 wk. Results are expressed as means ± SEM; n = 5–6 mice per group. Two-way ANOVA, Bonferroni posttests: * $P < 0.05$, ** $P < 0.01$, *** $P < 0.001$.

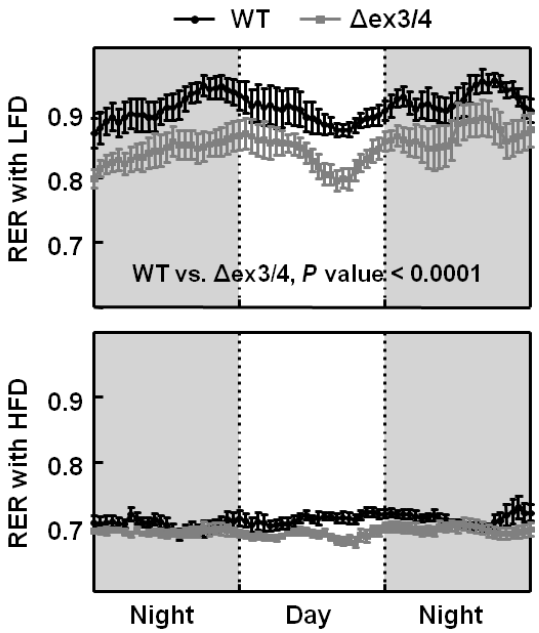

Figure 17. The metabolism in the Nr1d1 Δex3/4 was changed to lipid utilization.

RER during night and day cycles were calculated by indirect calorimetry. Shaded area indicates the dark period (active / feeding time). Values are expressed as means as means ± SEM; n =6–8 mice per group. Two-way ANOVA test, Bonferroni posttests.

3.2.2. The severe liver injuries in the Nr1d1 Δex3/4 mice after HFD feeding

It was evaluated whether the deletion of exons 3 and 4 in *Nr1d1* in response to HFD-induced obesity affects the physiology of livers. First, the liver weights were measured at the end of experiments for 12 weeks diets. Fatty liver disease causes an abnormally enlarged liver, termed as hepatomegaly [Cohen et al., 2011]. The livers weight in both HFD-fed WT and Nr1d1 Δex3/4 mice were significantly increased compared to the LFD-fed WT mice, and the hepatomegaly of the Nr1d1 Δex3/4 mice was more developed than that of the WT mice with HFD feeding (Figure 18).

Next, hematoxylin and eosin (H&E) staining of liver sections was assessed (Figure 19). Livers from the LFD-fed WT and Nr1d1 Δex3/4 mice showed normal hepatocytes architecture and no evidence of steatosis. However, both the WT and the Nr1d1 Δex3/4 mice developed hepatic steatosis after the HFD feeding. H&E staining showed that the liver tissues from both WT and the Nr1d1 Δex3/4 mice displayed lipid droplet accumulation and ballooning in hepatocytes after HFD feeding. The Nr1d1 Δex3/4 mice showed more severe hepatic steatosis with more extensive lipid droplet deposition of macrovesicles and ballooning in the hepatocytes.

The severity of steatosis in the liver is associated with liver inflammation, and the serum levels of ALT and AST are indicative for increased liver injuries

[Hardy et al., 2016]. The serum levels of ALT and AST were largely increased in the Nr1d1 Δex3/4 mice compared to the Nr1d1 WT mice after the HFD feeding (Figure 20). Additionally, abnormal liver function due to non-alcoholic fatty liver disease (NAFLD) is common in diabetes [Armstrong et al., 2014]. The serum glucose showed higher values in the Nr1d1 Δex3/4 mice compared to the Nr1d1 WT mice in LFD feeding, suggesting altered glucose basal homeostasis (Figure 21). Of course, the Nr1d1 Δex3/4 mice displayed hyperglycemia as well as the Nr1d1 WT mice in HFD feeding.

Together, these observations suggest that the liver injuries seen in the HFD-fed Δex3/4 mice are the result of the genetic susceptibility in response to systemically metabolic challenge.

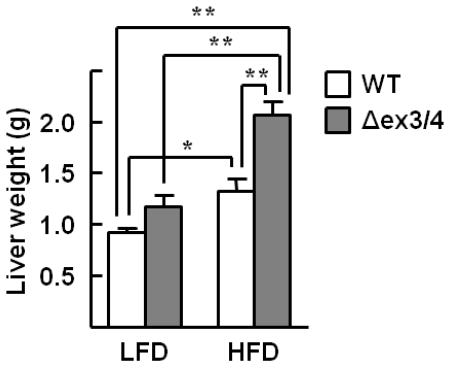

Figure 18. The hepatomegaly of the Nr1d1 Δex3/4 mice was more developed than that of the WT mice with HFD feeding.

Liver weights were measured when liver tissues were excised after blood collection. Results are expressed as means ± SEM; n = 5–6 mice per group. *P < 0.05, **P < 0.01.

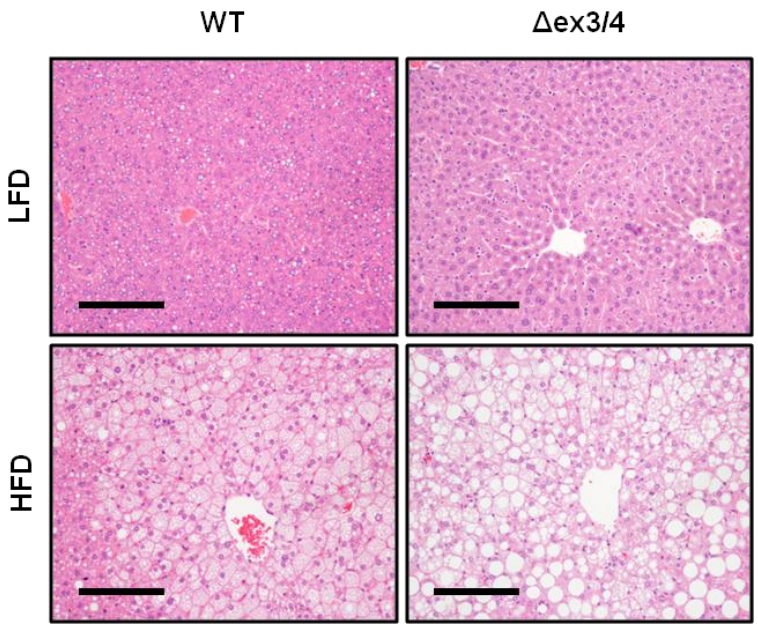

Figure 19. Representative image of hepatic hematoxylin and eosin (H&E) staining after diet challenges.

Liver tissues obtained from the WT and the Nr1d1 Δex3/4 mice fed either LFD or HFD were subjected to H&E staining. Representative images are shown (200X magnification). Scale bar: 50 μm.

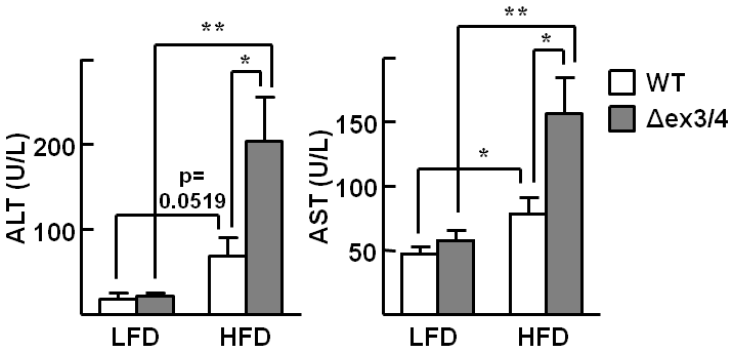

Figure 20. Effect of the HFD feeding on serum levels of liver enzymes in the Nr1d1 Δex3/4.

Serum AST and ALT levels were measured by standard clinical chemistry assays. Values represent mean ± SEM (n=5-7), * $P < 0.05$, ** $P < 0.01$.

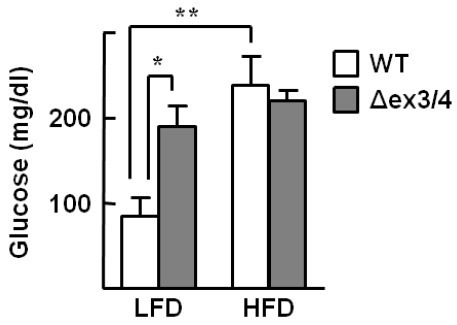

Figure 21. Effect of the HFD feeding on serum glucose levels in the Nr1d1 Δex3/4.

Serum glucose levels were measured by standard clinical chemistry assays. Values represent mean ± SEM (n=5-7), * $P < 0.05$, ** $P < 0.01$.

3.2.3. The enhanced HFD-induced hepatic steatosis in the Nr1d1 Δex3/4 mice

In accordance with these observations, liver triglycerides (TGs) levels were determined. The HFD feeding in the Nr1d1 Δex3/4 mice dramatically induced hepatic steatosis, which was evidenced by H&E staining of liver sections and confirmed by ORO staining. ORO staining, which is intended for use in the histological visualization of fat cells and neutral fat, showed lipid droplet accumulation in the Nr1d1 Δex3/4 mice after HFD feeding (Figure 22). In particular, the lipid droplets in the HFD-fed Nr1d1 Δex3/4 mouse livers were larger and denser than that in the HFD-fed WT livers.

Similarly, the levels of hepatic TGs in the HFD-fed Nr1d1 Δex3/4 mice were higher than that in the HFD-fed WT mice (Figure 23). The hepatic TG concentration in the HFD-fed Nr1d1 Δex3/4 mice exceeded 62 mg/g liver compared to the HFD-fed WT mice, and the concentration was clinically defined as hepatic steatosis by. In spite of a tendency toward higher hepatic TG levels in the Nr1d1 Δex3/4 mice, the serum TG levels in the Nr1d1 Δex3/4 mice made no significant difference to that of the Nr1d1 WT mice after HFD feeding (Figure 24). Serum total cholesterol levels were measured as an indication of other lipid profiles, and the levels in the HFD-fed Nr1d1 Δex3/4 mice were significantly increased compared to those in the HFD-fed Nr1d1 WT mice (Figure 25). These results demonstrated that the Nr1d1 Δex3/4 mice showed more severe HFD-induced hepatic steatosis than the WT mice.

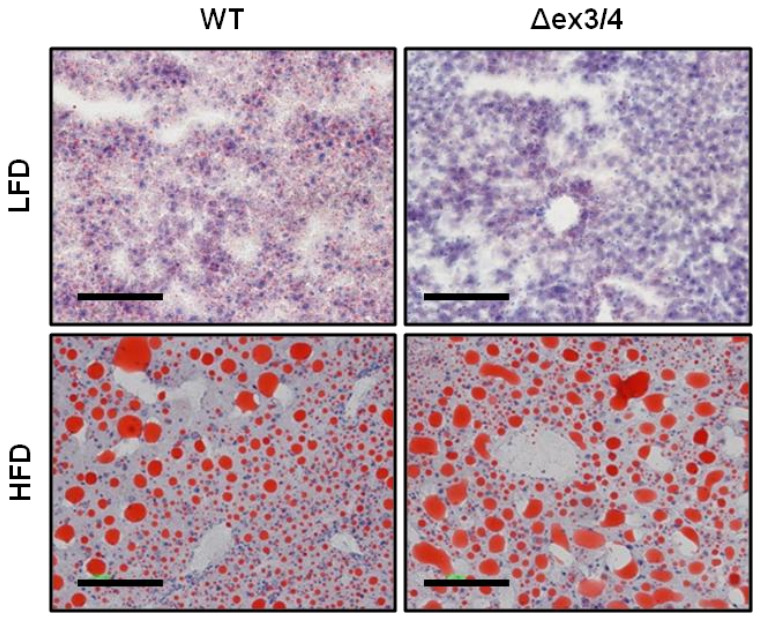

Figure 22. Representative image of hepatic oil-red o (ORO) staining after diet challenges.

Frozen livers from the indicated mice were subjected to ORO staining. Representative images are shown (200X magnification). Scale bar: 50 μm.

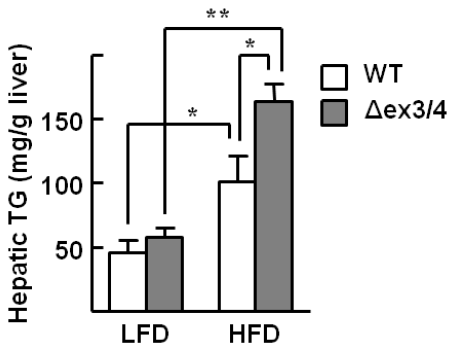

Figure 23. Effect of the HFD feeding on hepatic TG accumulation in the Nr1d1 Δex3/4.

Hepatic TG was measured by glycerol assays. Values represent mean ± SEM (n=5-7), * $P < 0.05$, ** $P < 0.01$.

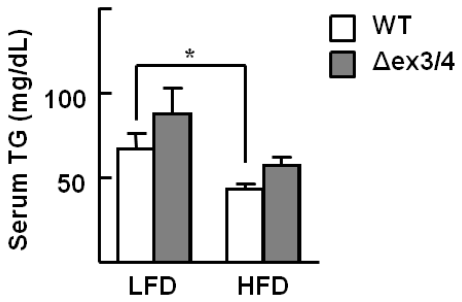

Figure 24. Effect of the HFD feeding on serum TGs levels in the Nr1d1 Δex3/4.

Serum TG levels were measured by standard clinical chemistry assays. Values represent mean ± SEM (n=5-7), * $P < 0.05$.

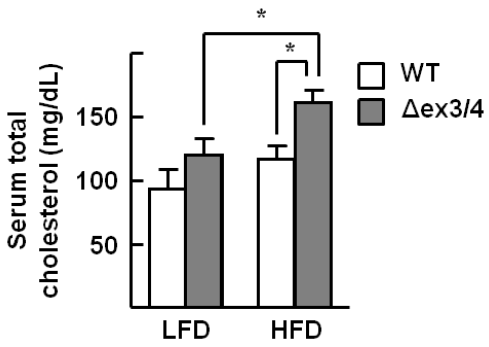

Figure 25. Effect of the HFD feeding on serum total cholesterol levels in the Nr1d1 Δex3/4.

Serum total cholesterol levels were measured by standard clinical chemistry assays. Values represent mean ± SEM (n=5-7), * $P < 0.05$.

3.3. Expression of hepatic genes in the Nr1d1 Δex3/4 mice after HFD feeding

3.3.1. Expression of metabolic genes is disrupted in the Nr1d1 Δex3/4 mice

To gain further insight into the role of the Nr1d1 as transcriptional factor for the regulation of hepatic metabolism, expressions of the metabolic genes in the liver were examined using RT-qPCR method. First, it was determined whether the HFD-induced defective energy homeostasis was associated with Nr1d1 expression. Notably, hepatic expression of the *Nr1d1* WT gene was significantly diminished in HFD feeding, while no significant difference was found for the *Nr1d1* Δex3/4 gene (Figure 26). In keeping with an observation that the deletion of the DBD in the *Nr1d1* gene worsened the hepatic steatosis, HFD markedly changed the expression of the *Nr1d1* WT gene, and might induce the hepatic steatosis.

Next, hepatic expression of lipogenic genes such as *sterol regulatory element binding transcription factor-1c* (*Srebp-1c*), *fatty acid synthase* (*Fasn*), *stearoyl-CoA desaturase 1* (*Scd1*), and *acetyl-CoA carboxylase 1* (*Acc1*) showed increased levels in the LFD-fed Nr1d1 Δex3/4 mice. However, the HFD did not induce the significant differences in expression of the lipogenic genes between two genotypes (Figure 27). In addition, hepatic cholesterol biosynthetic genes (e.g., *sterol regulatory element binding transcription factor 2* (*Srebf2*), *3-hydroxy-3-methylglutaryl-CoA reductase* (*Hmgcr*), and *farnesyl-*

diphosphate farnesyltransferase 1 (*Fdft1*)) did not exhibit the changed expression levels in the liver of the Nr1d1 Δex3/4 mice regardless of diets (Figure 28). The mRNA levels of *3-hydroxy-3-methylglutaryl-CoA synthase 1* (*Hmgcs1*), which encodes the rate-limiting enzyme in cholesterol biosynthesis, was increased in the LFD-fed Nr1d1 Δex3/4 compared to the LFD-fed Nr1d1 WT mice. Of interest, the fatty acid transporter, *cluster of differentiation 36* (*Cd36*), also known as *Fat* (*fatty acid translocase*) was induced by the Nr1d1 Δex3/4, or by HFD, while *solute carrier family 27 member 1* (*Slc27a1*), which encodes long-chain fatty acid transport protein 1 across plasma membrane, was not induced (Figure 29).

Taken together, the lipid-associated metabolic genes of the Nr1d1 Δex3/4 mice in the liver were somewhat increased in LFD feeding, but seemed to be fully induced and showed no critical difference in HFD feeding. Although the responses of the Nr1d1 Δex3/4 mice to HFD were associated with triglyceride synthesis, fatty acid uptake and cholesterol synthesis in the liver, the gene expression levels did not distinguish from the crucial pathways as the causes of the enhanced hepatosteatosis.

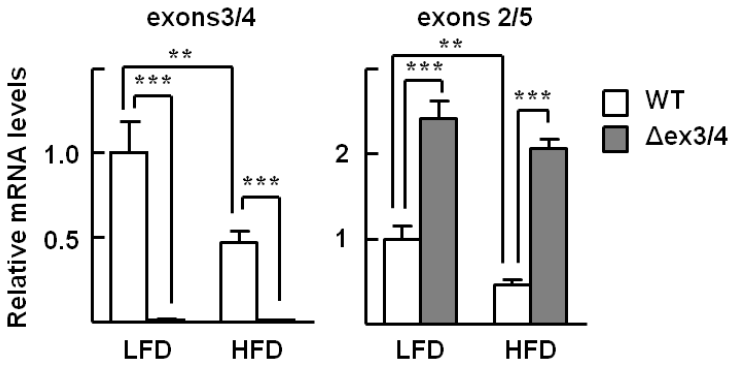

Figure 26. Hepatic mRNA expression of the *Nr1d1* gene in the WT and the Nr1d1 Δex3/4 mice.

Hepatic mRNA expression levels of the WT and the Nr1d1 Δex3/4 mice were measured by RT-qPCR using different sets of primers as indicated. Values represent mean ± SEM (n=6-9). ** $P < 0.01$ and *** $P < 0.001$.

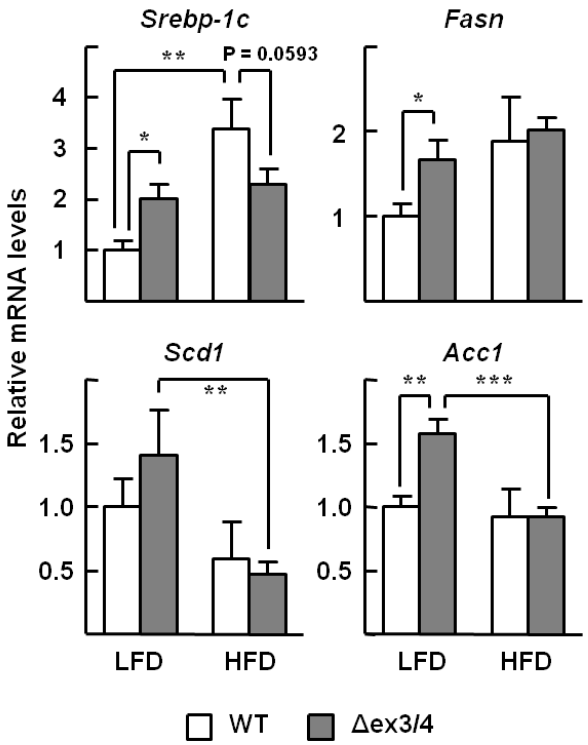

Figure 27. The mRNA expression of lipogenic genes in the liver of the WT and the Nr1d1 Δex3/4 mice.

The mRNA expression levels of the lipogenic genes in the WT and the Nr1d1 Δex3/4 mice were measured by RT-qPCR. Values represent mean ± SEM (n=6-8). * $P < 0.05$ and ** $P < 0.01$.

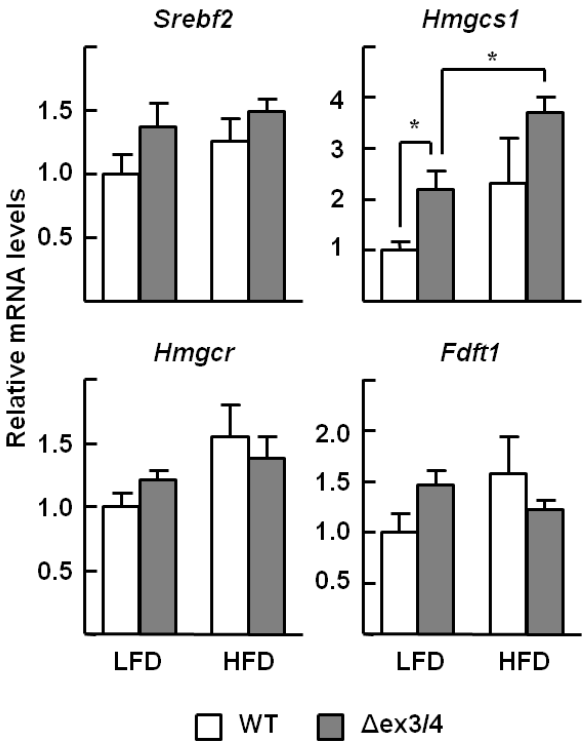

Figure 28. The mRNA expression of cholesterol biosynthetic genes in the liver of the WT and the Nr1d1 Δex3/4 mice.

The mRNA expression levels of the cholesterol biosynthetic genes in the WT and the Nr1d1 Δex3/4 mice were measured by RT-qPCR. Values represent mean ± SEM (n=6-8). * $P < 0.05$ and ** $P < 0.01$.

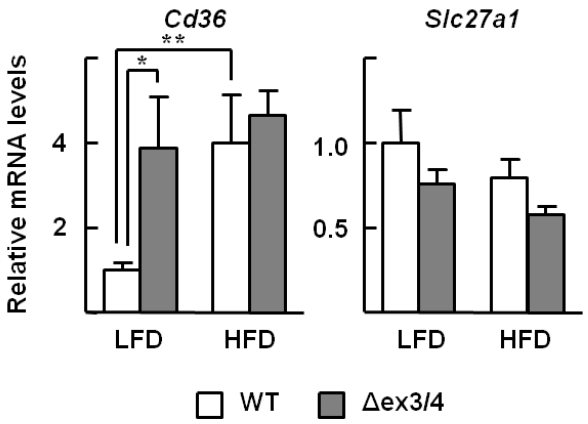

Figure 29. The mRNA expression of lipid uptake genes in the liver of the WT and the Nr1d1 Δex3/4 mice.

The mRNA expression levels of the lipid uptake genes in the WT and the Nr1d1 Δex3/4 mice were measured by RT-qPCR. Values represent mean ± SEM (n=6-8). * $P < 0.05$ and ** $P < 0.01$.

3.3.2. Expression of inflammatory genes is disrupted in the Nr1d1 Δex3/4 mice

To further specify the liver injuries of the Nr1d1 Δex3/4 mice, the mRNA levels of inflammatory genes were analyzed in the liver (Figure 30). *Interleukin-6* (*Il-6*) was significantly downregulated by HFD in both genotypes as well as LFD-fed Nr1d1 WT mice. Incidentally, hepatic expression of *tumor necrosis factor alpha* (*Tnfα*) and *nitric oxide synthase type II* (*Nos2*) were altered by the *Nr1d1* Δex3/4 genotype in both diets. Specially, increased levels of *Tnfα* supported the elevated ALT and AST levles in HFD-fed Nr1d1 Δex3/4 mice. As such, altered expression of inflammatory cytokine genes would have contributed to lead the HFD-induced hepatic steatosis to steatohepatitis in the Nr1d1 Δex3/4 mice.

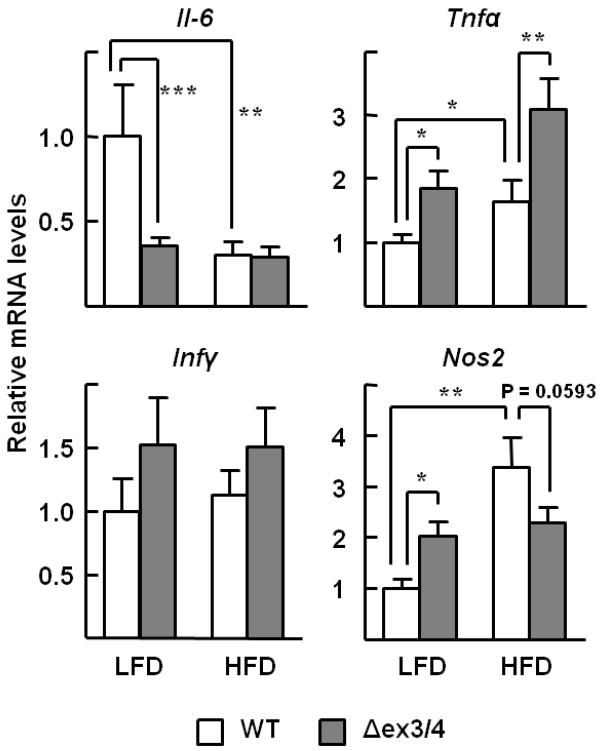

Figure 30. The mRNA expression of inflammatory cytokine genes in the liver of the WT and the Nr1d1 Δex3/4 mice.

The mRNA expression levels of the inflammatory cytokine genes in the WT and the Nr1d1 Δex3/4 mice were measured by RT-qPCR. Values represent mean ± SEM (n=6-8). * $P < 0.05$, ** $P < 0.01$, and *** $P < 0.001$.

3.4. Gene expression profiling in the Nr1d1 Δex3/4 mice after HFD feeding

3.4.1. Differential hepatic gene expression analysis

To figure out the detailed transcriptomic alterations in response to the deletion of Nr1d1 exons 3 and 4 and HFD feeding, microarray analysis was performed. The transformed and normalized data were compared using two-way ANOVA ($P < 0.05$) and filtered by fold change (cutoff; > 1.5) to assess differences between diets and genotypes. After the unknown or duplicated probe sets had been removed, 204 genes by diet effect, 67 genes by genotype effect and 163 genes by interaction effect (a total of 408) were identified as differentially expressed genes. Diet affected the differential gene expression more than genotype. One gene, *thyroid hormone-responsive* (*Thrsp*) and one *microRNA*, (*Mir103-2*) displayed in common for all three types of effects. Among 210 genes by diet effect, 86 genes were upregulated, and 124 genes were downregulated. Among 67 genes by genotype effect, 39 genes were upregulated, and 28 genes were downregulated (Figure 31).

To visualize the difference of the deletion of *Nr1d1* exons 3 and 4 between LFD and HFD, the gene set list affected by interaction effect was selected to generate a heat map (Figure 32). The resulting color indicates that the LFD-fed Nr1d1 WT mice showed a distinct gene expression pattern from the other group mice.

To further investigate these data, the Toppgene tool was used to functionally cluster up- and down-regulated genes by similarly annotated gene ontology (GO) biological process terms in gene sets from the diet and genotype effect, respectively. The gene set from interaction effect was totally clustered. The results of functional annotation analysis are shown in Table 3, 4 and 5. The clusters with the upregulated gene sets from diet effects were related to the unfolded protein response, and the clusters with the downregulated gene sets from diet effects were mainly related to lipid metabolism. Of interesting, the genotype affected the upregulation of triglyceride metabolic genes and the downregulation of glutathione synthetic genes. The gene sets from interaction effect was associated with neutrophil homeostasis and cyclic adenosine monophosphate (cAMP) metabolism.

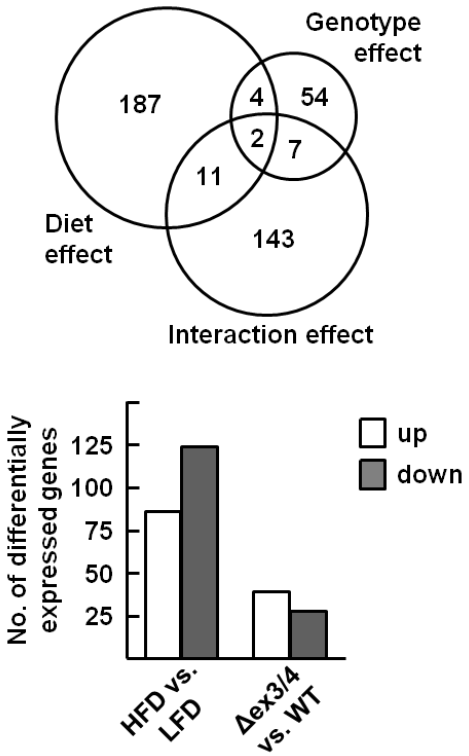

Figure 31. Differential expressed genes in the Nr1d1 Δex3/4 mice after HFD feeding.

Venn diagram for abundances of gene affected by diet, genotype, and interaction effects (up). The numbers of statistically significant up- and downregulated genes affected by diet and genotype effects (down).

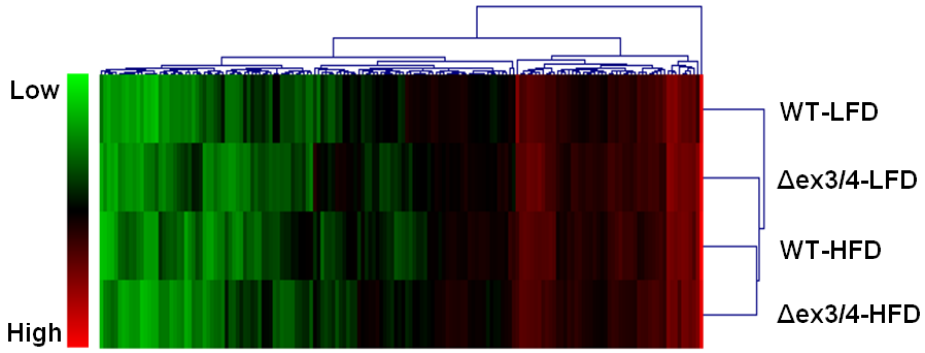

Figure 32. Dendrogram for hierarchical clustering of genes and samples in the Nr1d1 Δex3/4 mice after HFD feeding.

Heat map showing the relative expression level for the gene set list affected by interaction effect based on differential gene expression data analysis. Hierarchical clustering of genes and samples was shown in the dendrogram on the top and side of the heat map using the Euclidean distance with complete linkage approach. The color scale represents gene expression levels: red is high level; green is low level.

Table 3. GO biological process top annotations in differentially expressed gene sets by diet effect.

Expression	GO Biological process annoations	Hits	P-value
Up	response to unfolded protein	8	2.22E-09
	response to topologically incorrect protein	8	3.45E-09
	endoplasmic reticulum unfolded protein response	7	8.26E-09
	cellular response to unfolded protein	7	9.69E-09
	cellular response to topologically incorrect protein	7	1.45E-08
	response to endoplasmic reticulum stress	7	1.07E-06
	cellular response to biotic stimulus	6	3.10E-06
	ER-associated ubiquitin-dependent protein catabolic process	4	1.32E-05
	ERAD pathway	4	2.98E-05
Down	carboxylic acid metabolic process	32	6.97E-18
	oxoacid metabolic process	32	1.43E-16
	organic acid metabolic process	32	2.21E-16
	carboxylic acid catabolic process	17	1.82E-15
	organic acid catabolic process	17	1.82E-15
	fatty acid metabolic process	20	2.76E-15
	monocarboxylic acid metabolic process	24	2.81E-15
	lipid metabolic process	33	8.01E-15
	small molecule catabolic process	18	3.04E-13
	cellular lipid metabolic process	27	1.15E-12
	lipid biosynthetic process	21	1.14E-11
	monocarboxylic acid catabolic process	11	1.83E-11
	cellular lipid catabolic process	13	1.90E-11

Table 3. ***Continued***

Expression	GO Biological process annoations	Hits	P-value
	lipid catabolic process	15	2.72E-11
	single-organism biosynthetic process	32	4.80E-11
	unsaturated fatty acid metabolic process	10	2.92E-10
	small molecule biosynthetic process	18	4.19E-10
	organic acid biosynthetic process	14	5.44E-10
	carboxylic acid biosynthetic process	14	5.44E-10
	long-chain fatty acid metabolic process	9	6.09E-10
	monocarboxylic acid biosynthetic process	12	8.21E-10
	single-organism catabolic process	24	9.48E-10
	fatty acid catabolic process	9	1.21E-09
	oxidation-reduction process	21	1.62E-08
	fatty acid oxidation	8	3.42E-08
	lipid oxidation	8	4.01E-08
	cellular catabolic process	28	4.22E-08
	lipid modification	11	5.94E-08
	cellular ketone metabolic process	11	6.70E-08
	organic substance catabolic process	28	1.07E-07
	serine family amino acid catabolic process	4	1.89E-07
	alpha-linolenic acid metabolic process	4	4.06E-07
	triglyceride catabolic process	5	4.32E-07
	L-cysteine metabolic process	3	4.84E-07
	cysteine catabolic process	3	4.84E-07
	L-cysteine catabolic process	3	4.84E-07

Table 3. ***Continued***

Expression	GO Biological process annoations	Hits	P-value
	steroid metabolic process	11	5.12E-07
	alpha-amino acid catabolic process	7	6.87E-07
	fatty acid biosynthetic process	8	6.96E-07
	organic hydroxy compound metabolic process	14	1.01E-06
	linoleic acid metabolic process	4	1.02E-06
	neutral lipid catabolic process	5	1.08E-06
	acylglycerol catabolic process	5	1.08E-06
	positive regulation of fatty acid metabolic process	5	1.24E-06
	fatty acid beta-oxidation	6	1.47E-06
	sulfur compound biosynthetic process	9	1.58E-06
	cellular amino acid catabolic process	7	1.88E-06
	steroid biosynthetic process	8	2.39E-06
	sulfur compound metabolic process	11	5.94E-06
	glycerolipid catabolic process	5	6.08E-06
	regulation of fatty acid metabolic process	6	9.71E-06
	sulfur amino acid catabolic process	3	9.97E-06
	fatty acid derivative metabolic process	6	1.22E-05
	icosanoid metabolic process	6	1.22E-05
	unsaturated fatty acid biosynthetic process	5	1.46E-05
	regulation of fatty acid oxidation	4	1.90E-05
	cysteine metabolic process	3	1.95E-05

The gene lists were also subjected to functional annotation analysis using ToppGene Suite with P-value (Bonferroni) < 0.05 and FDR < 0.05 correction.

Table 4. GO biological process top annotations in differentially expressed gene sets by genotype effect.

Expression	GO Biological process annoations	Hits	P-value
Up	triglyceride metabolic process	4	2.44E-05
	acylglycerol metabolic process	4	3.82E-05
	neutral lipid metabolic process	4	3.94E-05
Down	glutathione derivative biosynthetic process	2	5.86E-05
	glutathione derivative metabolic process	2	5.86E-05

The gene lists were also subjected to functional annotation analysis using ToppGene Suite with P-value (Bonferroni) < 0.05 and FDR < 0.05 correction.

Table 5. GO biological process top annotations in differentially expressed gene sets by interaction effect.

Expression	GO Biological process annoations	Hits	P-value
Up or down	neutrophil homeostasis	3	3.64E-05
	cAMP catabolic process	3	8.98E-05
	cyclic nucleotide catabolic process	3	1.38E-04

The gene lists were also subjected to functional annotation analysis using ToppGene Suite with P-value < 0.05 and FDR < 0.08 correction.

3.4.2. Prediction of upstream regulators for altered hepatic gene expression in the Nr1d1 Δex3/4 mice after HFD feeding

To better understand the molecular mechanisms for the changes in gene expression, we analyzed enrichment of TFBSs [Kwon et al., 2012]. Since the Nr1d1 Δex3/4 protein had no DBD and its transcriptional activity disappeared in these Nr1d1 Δex3/4 mice model, the transcriptomic alteration would be resulted from some transcriptional factors. The gene set lists that was differentially expressed in the diet, genotype, and interaction effects, respectively, revealed 10 overrepresented transcription factors ranked by Z-score (Table 6).

As the deletion of exons 3 and 4 in the *Nr1d1* responded the HFD feeding, and showed the hepatic steatosis phenotype, the transcription factors predicted in the interaction effect were focused. Among these transcription factors, CCAAT/enhancer-binding protein alpha (Cebpα) and hepatocyte nuclear factor 4 alpha (Hnf4α) are enriched in liver and well characterized for their functions in lipid homeostasis [Hayhurst et al., 2001; Ramji et al., 2002]. Consistently, analysis with the Cytoscape plug-in GeneMANIA software showed that networks of genes that coexpressed with Cebpα and Hnf4α were associated with hepatic genes involved in the regulation of lipid biosynthesis and glucose metabolism (Figure 33 and 34) [Warde-Farley et al., 2010].

Table 6. Significantly overrepresented TFBSs for differentially expressed gene sets.

Diet effect			**Genotype effect**			**Interaction effect**		
TF	Hits	Z-score	TF	Hits	Z-score	TF	Hits	Z-score
Tcfcp2l1	81	14.667	FOXF2	13	13.87	HLF	20	11.42
NFYA	49	10.775	TEAD1	18	12.475	Tal1::Gata1	27	9.53
NR2F1	34	10.414	Pax4	1	10.843	Pax4	1	7.377
STAT1	50	8.582	CTCF	10	9.482	Ddit3::Cebpa	23	7.058
Myf	80	8.128	Gfi	36	8.984	EBF1	48	6.456
MYC::MAX	27	7.565	NFE2L2	20	8.598	TAL1::TCF3	31	5.931
PPARG::RXRA	41	7.536	NFYA	16	7.592	znf143	7	5.782
RUNX1	107	7.003	NR2F1	10	7.162	Sox2	10	4.497
HNF4A	53	6.978	REL	29	5.711	HNF4A	28	4.48
NR4A2	109	6.935	Sox17	37	5.388	USF1	37	4.455

Top ten overrepresented conserved TFBSs were ranked by Z-score which reflects the occurrence of the TFBS in the promoters of the target gene set compared to background gene set.

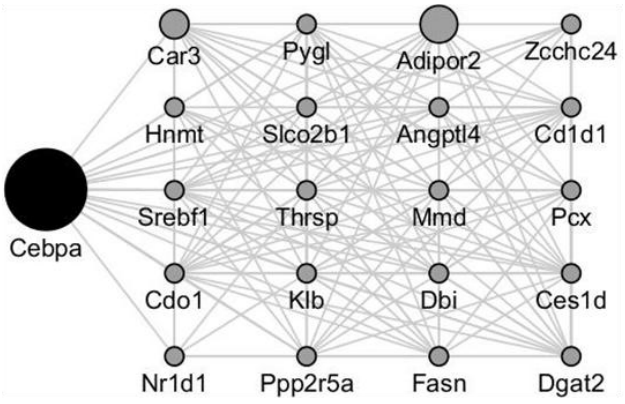

GO function	Hits	Q-value
Neutral lipid metabolic process	5	1.4E-04
Acylglycerol metabolic process	5	1.4E-04
Regulation of lipid metabolic process	6	4.6E-04
Triglyceride metabolic process	4	2.8E-03
Glycerolipid metabolic process	5	5.9E-03
Triglyceride biosynthetic process	3	5.9E-03

Figure 33. Cebpα was predicted as an upstream regulator for altered hepatic gene expression in the Nr1d1 Δex3/4 mice after HFD feeding.

The networks of twenty genes that co-expressed with Cebpα in the liver was predicted by Cytoscape plug-in GeneMANIA (up). Top ranked gene ontology (GO) functional annotations with the significance. Q-value was calculated by a FDR corrected hypergeometric test for enrichment (low).

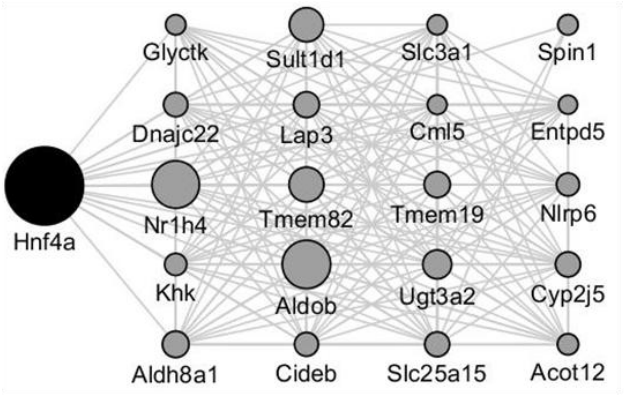

GO function	Hits	Q-value
Regulation of carbohydrate metabolic process	4	0.16
Hexose metabolic process	4	0.21
Glucose metabolic process	4	0.21
Monosaccharide metabolic process	4	0.21
Regulation of glucose metabolic process	3	0.54

Figure 34. Hnf4α was predicted as an upstream regulator for altered hepatic gene expression in the Nr1d1 Δex3/4 mice after HFD feeding.

The networks of twenty genes that co-expressed with Hnf4α in the liver was predicted by Cytoscape plug-in GeneMANIA (up). Top ranked gene ontology (GO) functional annotations with the significance. Q-value was calculated by a FDR corrected hypergeometric test for enrichment (low).

3.4.3. A putative target gene associated with function of HFD-responsive Nr1d1

Expression of *Thrsp*, which displayed all three types of effects, was further analyzed to confirm the results of the microarray analysis. Consistently, the hepatic mRNA expression level of *Thrsp* was significantly altered in different genotypes and different diets. It was most strikingly changed by genotype together with diet (Figure 35). In addition, the Cytoscape plug-in GeneMANIA analysis showed significant gene ontology annotations of the 20 genes that were predicted to coexpress with *Thrsp* were associated with fatty acid metabolism (Figure 36). Thus, these results indicate that these differentially expressed genes could represent the fat-prone hepatic phenotype in the Nr1d1 Δex3/4 mice after HFD feeding.

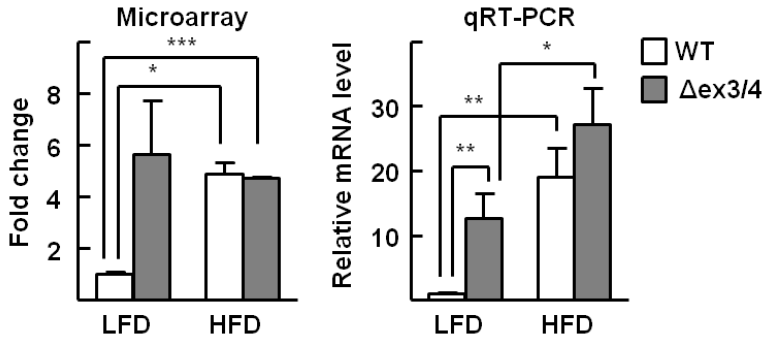

Figure 35. Expression of *Thrsp* in the livers of the Nr1d1 Δex3/4 mice.

Relative expression of *Thrsp* in microarray was shown. Values represent mean ± SEM (n=2), * $P < 0.05$, *** $P < 0.001$ (left). Relative hepatic mRNA level of Thrsp gene was determined by RT-qPCR and normalized with 18S rRNA. mRNA expression value of LFD-fed WT was set as 1.0. Values represent mean ± SEM (n=6-8), * $P < 0.05$, ** $P < 0.01$(right).

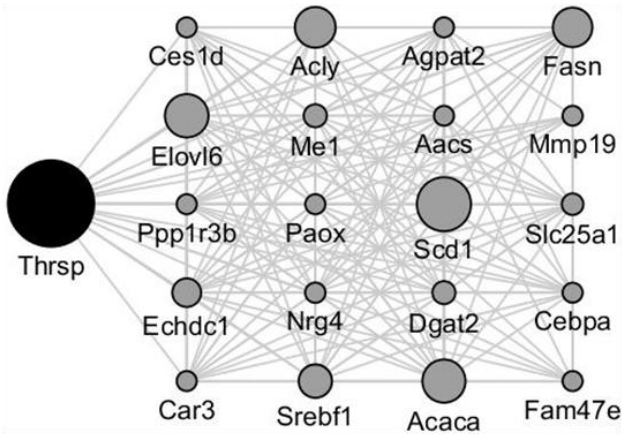

GO function	Hits	Q-value
Fatty acid biosynthetic process	5	5.0E-04
Fatty acid metabolic process	6	8.4E-04
Monocarboxylic acid biosynthetic process	5	1.1E-03
Thioester metabolic process	4	1.2E-03
Acyl-CoA metabolic process	4	1.2E-03

Figure 36. The coexpressed gene network of *Thrsp* and its functional annotation analysis.

The network of twenty genes that coexpressed with *Thrsp* was predicted by Cytoscape plug-in GeneMANIA (up). Top ranked GO functional annotations with the significance. Q-value was calculated from a FDR corrected hypergeometric test for enrichment (low).

3.5. The hepatic steatosis in liver-specific *Nr1d1* Δex3/4 mice

3.5.1. The generation of liver-specific Nr1d1 Δex3/4 mice

In this study, the deletion of exons 3 and 4 in the *Nr1d1* worsened the hepatic steatosis in response to HFD, and alternative transcription factors like Cebpα and Hnf4α were somehow involved in the various lipid metabolism pathways including fatty acid synthesis, and triglyceride metabolism. To further investigate whether these physiological effects was resulted from the Nr1d1 of hepatocytes, the exons 3 and 4 of *Nr1d1* were liver-specifically deleted in mice by crossing the *Nr1d1* floxed mice with transgenic albumin (Alb)-cre deleter mice [Lee et al., 2016]. The mice are called as the Nr1d1 LΔex3/4 mice. The breeding scheme and the result of genotyping are in Figure 37.

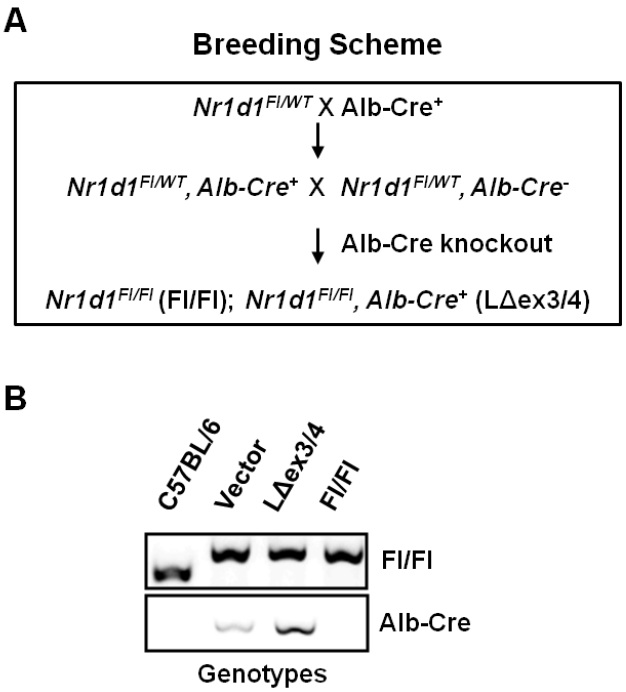

Figure 37. The breeding scheme and genotyping of the Nr1d1 LΔex3/4.

(A) The Nr1d1 floxed mice were crossed with the Alb-Cre mice. (B) Targeted deletion of the Nr1d1 in hepatocytes. Genotyping Fl/Fl (the Nr1d1 floxed allele) and LΔex3/4 littermates was performed by PCR using specific primers as indicated.

3.5.2. The little difference of HFD-induced hepatic steatosis in the Nr1d1 LΔex3/4 mice

To test the function of the hepatic *Nr1d1* gene in the pathogenesis of NAFLD, the 7-week-old male Fl/Fl and Nr1d1 LΔex3/4 mice were fed with LFD or HFD for 12 weeks. Similar to the Nr1d1 Δex3/4 mice, the body weights of 7-week-old Nr1d1 LΔex3/4 mice were different from those of the Nr1d1 Fl/Fl mice. At the end of the HFD feeding of 10 weeks, the HFD-fed Fl/Fl and LΔex3/4 mice were significantly heavier than both the LFD-fed Fl/Fl and the Nr1d1 LΔex3/4 mice. However, in HFD feeding groups, there was not the body weight change between the Fl/Fl and the Nr1d1 LΔex3/4 mice (Figure 38). It indicated that the hepatic disruption of the Nr1d1 did not induce the severity in the metabolic alterations in response to HFD-induced obesity.

Next, the liver weights were measured at the end of experiments for 12 weeks diets. While the livers weight in both HFD-fed Fl/Fl and Nr1d1 LΔex3/4 mice were significantly increased compared to the LFD-fed Fl/Fl mice, the hepatomegaly of the Nr1d1 LΔex3/4 mice did not occur with HFD feeding (Figure 39).

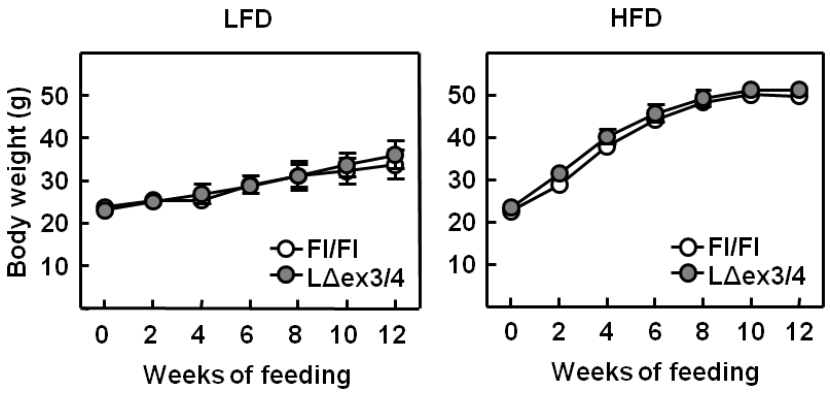

Figure 38. The body weights of Nr1d1 LΔex3/4 mice are not susceptible to the HFD feeding.

Body weights were measured every other weeks in the Fl/Fl and the Nr1d1 LΔex3/4 mice fed a LFD or a HFD for 12 wk. Results are expressed as means ± SEM; n = 6–8 mice per group.

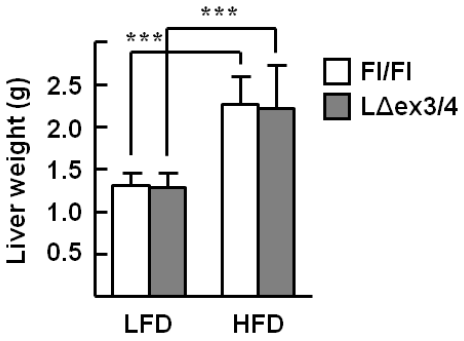

Figure 39. The hepatomegaly of the Nr1d1 LΔex3/4 mice was not developed than that of the WT mice with HFD feeding.

Liver weights were measured when liver tissues were excised after blood collection. Results are expressed as means ± SEM; n = 6–8 mice per group. *** $P < 0.001$.

In addition, H&E staining of liver sections showed that livers from the LFD-fed mice groups regardless of genotypes have normal hepatocytes architecture and no evidence of lipid accumulation in the hepatocytes. However, both the Fl/Fl and the Nr1d1 LΔex3/4 mice developed the hepatic steatosis after the HFD feeding. The liver tissues from both the Fl/Fl and the Nr1d1 LΔex3/4 mice displayed lipid droplet accumulation in hepatocytes after HFD feeding, similarly between both genotypes (Figure 40).

It was consistent with ORO staining results that lipid droplet accumulation in the Nr1d1 LΔex3/4 mice was the same with the Nr1d1 Fl/Fl mice after HFD feeding (Figure 41). Besides, the levels of hepatic TGs in the HFD-fed Nr1d1 LΔex3/4 mice were similar to those in the HFD-fed Nr1d1 Fl/Fl mice (Figure 42).

Taken together, the HFD-induced obesity did not boost the hepatic steatosis in the Nr1d1 LΔex3/4 mice, unlike the whole-body knockout Nr1d1 Δex3/4 mice.

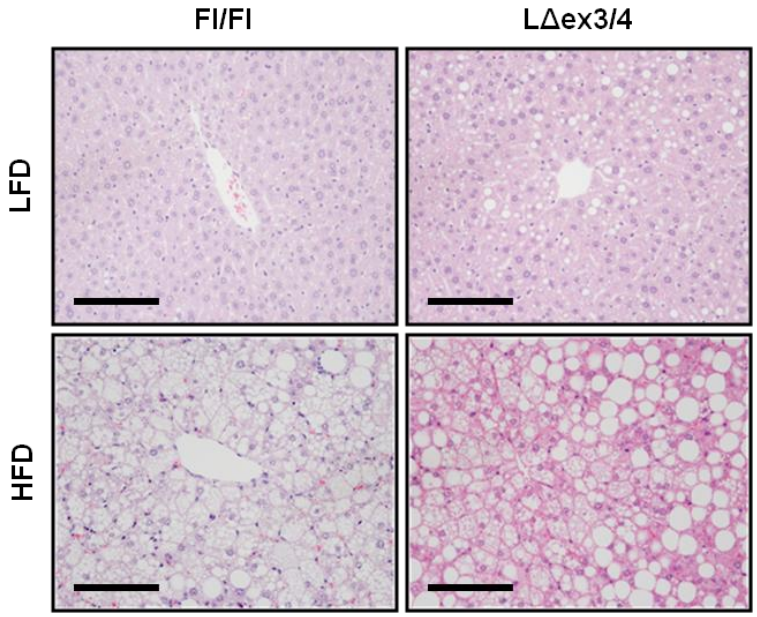

Figure 40. Representative image of hepatic H&E staining after diet challenges in the Nr1d1 LΔex3/4 mice.

Liver tissues obtained from the Fl/Fl and the Nr1d1 LΔex3/4 mice fed either LFD or HFD were subjected to H&E staining. Representative images are shown (200X magnification). Scale bar: 50 μm.

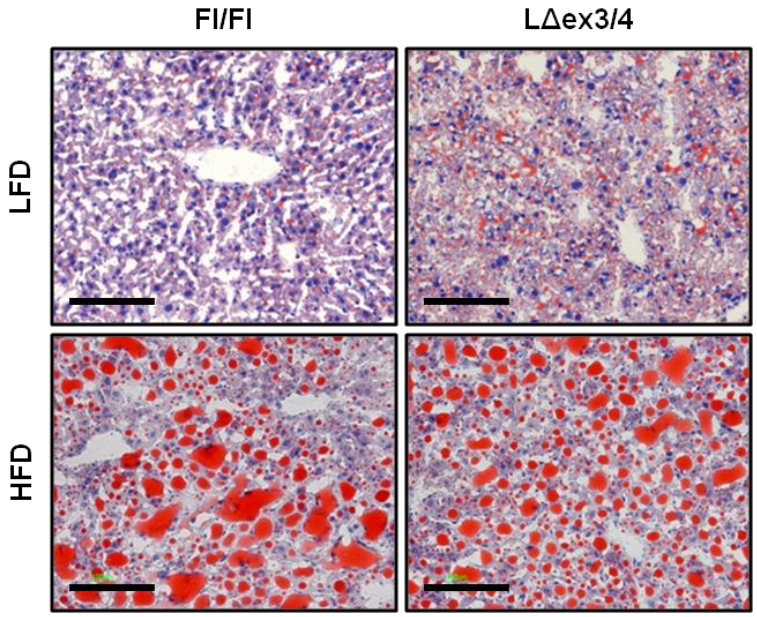

Figure 41. Representative image of hepatic ORO staining after diet challenges in the Nr1d1 LΔex3/4 mice.

Frozen livers from the indicated mice were subjected to ORO staining. Representative images are shown (200X magnification). Scale bar: 50 μm.

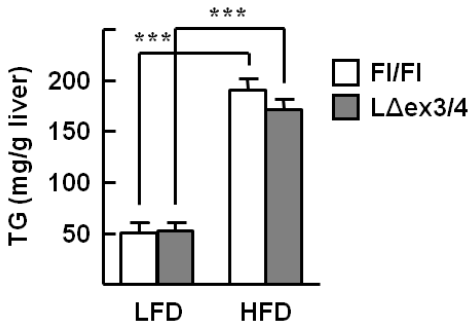

Figure 42. Effect of the HFD feeding on hepatic TG accumulation in the Nr1d1 LΔex3/4 mice.

Hepatic TG was measured by glycerol assays. Values represent mean ± SEM (n=6-8), *** $P < 0.001$.

3.5.3. The biochemical assessment of liver damage in the Nr1d1 LΔex3/4 mice after HFD feeding

To test the liver damage in the Nr1d1 LΔex3/4 mice after HFD feeding, the biochemical assessments were done by measuring the levels of ALT and AST. The serum levels of ALT and AST were largely increased in the HFD-fed mice groups compared to the LFD-fed mice groups (Figure 43). Additionally, the serum glucose also showed higher values in the HFD-fed mice groups compared to the LFD-fed mice groups (Figure 44). However, the HFD feeding did not induce the different levels of the serum enzymes and glucose, consistent of the same levels of hepatic steatosis between the Fl/Fl and the Nr1d1 LΔex3/4 mice even after HFD feeding.

By the way, the serum lipid profile revealed that the cholesterol metabolism in the Nr1d1 LΔex3/4 mice was altered in response to the HFD feeding. In particular, the total cholesterol levels of the Nr1d1 LΔex3/4 mice were increased compared to that of the Fl/Fl mice with the LFD feeding. However, the total cholesterol levels of the HFD-fed Nr1d1 LΔex3/4 mice remained the same with those of the HFD-fed Nr1d1 Fl/Fl mice (Figure 45).

Therefore, these data demonstrated that the hepatic steatosis seen in the HFD-fed LΔex3/4 mice is not the hepatocyte-specific result of the genetic susceptibility in response to systemically metabolic challenge.

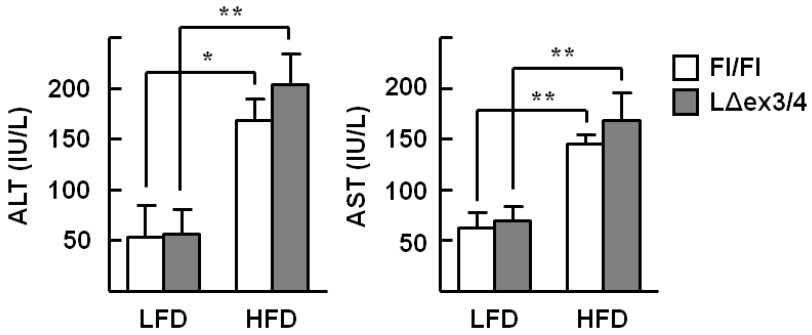

Figure 43. Effect of the HFD feeding on serum levels of liver enzymes in the Nr1d1 LΔex3/4.

Serum AST and ALT levels were measured by standard clinical chemistry assays. Values represent mean ± SEM (n=6-8), * $P < 0.05$, ** $P < 0.01$.

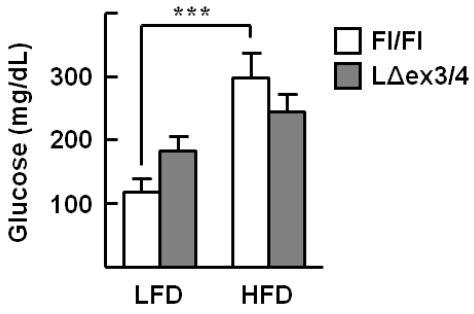

Figure 44. Effect of the HFD feeding on serum glucose levels in the Nr1d1 LΔex3/4.

Serum glucose levels were measured by standard clinical chemistry assays. Values represent mean ± SEM (n=6-8), *** $P < 0.001$.

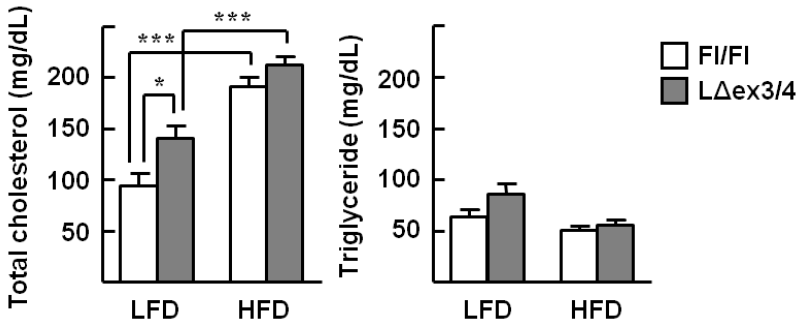

Figure 45. Effect of the HFD feeding on serum total cholesterol and TG levels in the Nr1d1 LΔex3/4.

Serum total cholesterol and TG levels were measured by standard clinical chemistry assays. Values represent mean ± SEM (n=6-8), * $P < 0.05$, *** $P < 0.001$.

4. Discussion

4.1. The importances of nuclear receptors in NAFLD

NAFLD is linked to chronic disturbances in lipid metabolism. Lipid homeostasis is mainly regulated by the liver which is an important ground organ for energy regulatory and immune pathways. Hepatic lipid metabolism is generally stimulated by nutrients and hormones, leading to balance metabolic requirements [Bechmann et al., 2012]. In addition to environmental stimuli, hepatic lipid homeostasis is modulated by genetic factors, especially various nuclear receptors such as the liver X receptors (LXRs), PPARs, FXR, and RAR-related orphan receptors (RORs) [Cave et al., 2016]. In the liver, these nuclear receptors has been studied basically to activate or repress target genes transcription by binding to their own specific DNA response elements to modulate cellular biological processes like bile acid synthesis, lipogenesis, lipoprotein metabolism, and fatty acid oxidation [López-Velázquez et al., 2012]. In addition, nuclear receptors have their specific ligands which can modulate the transcriptional activities of nuclear receptors. These ligands act as agonists and antagonist, and nuclear receptors can also partially bind to ligands. The ligand binding ability of nuclear receptor makes nuclear receptors good drug targets of human diseases. Recently, RORα, which shares a DNA response element with NR1D1 in a competition mode, was reported to play hepatoprotective roles via novel metabolic target genes, and its synthetic ligands was confirmed as an excellent modulator for NAFLD [Kim et al., 2012; Han et al., 2014]. Therefore, a detailed understanding of mechanism of action of nuclear receptors is required to drug discovery for NAFLD.

4.2. The strategic validity of the Nr1d1 Δex3/4 mice

Nr1d1 is a ligand-regulated nuclear receptor and transcriptional factor containing DBD that directly binds to specific DNA response elements like RevDR2 and RORE, and recruits corepressors such as nuclear receptor corepressor (NCoR) and histone deacetylase 3 (HDAC3) to repress target gene transcription [Harding and Lazar, 1995; Yin and Lazar, 2005]. In this aspect, a strategy which targets the exons encoding DBD, a mainly active domain of the protein, is appropriate for generation of the Nr1d1-disrupted mice model. Incidentally, the strategy consisted of deleting the exons 3 and 4, a part of region encoding DBD, allowing the generation of the DBD-deleted mice with a subsequent frame shift of the encoding sequence. The Nr1d1 Δex3/4 mice expressed an internally truncated Nr1d1 lacking the DBD. Since the Nr1d1 Δex3/4 protein was overexpressed in the cells, it was required to verify the strategic validity of the Nr1d1 Δex3/4 mice.

While the Nr1d1 protein is a nuclear protein, the Nr1d1 Δex3/4 protein was located in nucleus and cytoplasm, and the increased Nr1d1 Δex3/4 protein expression was observed excessively in cytoplasm (Figure 10-12). In previous report, DBD-deleted Nr1d1 has been observed in cytoplasmic localization, and the phenomenon is ascribed to a nuclear localization signal (NLS) in DBD [Chopin-Delannoy et al., 2003]. In this mouse model, the deletion of DBD led to loss a NLS in DBD, and the Nr1d1 Δex3/4 protein, in which a C-terminal part of DBD still remains, was subsequently distributed in both

nucleus and cytoplasm.

Another huge issue was that the Nr1d1 Δex3/4 mRNA and protein were overexpressed in the cells. Although the Nr1d1 Δex3/4 protein is partly located in nuclei, the expression levels of the protein as well as mRNA were elevated. The *Nr1d1* is a self-repressing gene which regulates the transcription itself as a repressor [Adelmant et al., 1996]. As a result, the self-repressing activity was released by the Nr1d1 Δex3/4, derepressing the transcription of the *Nr1d1*. Moreover, it can be assumed that the Nr1d1 has the ubiquitination region in the DBD. Generally, nuclear receptors have the ubiquitination region in the LBD, and the proteasomal degradation process is dependent on ligand binding to the nuclear recptors [Pawlak et al., 2012]. In contrast, the peroxisome proliferator-activated receptor (PPAR) β/δ has an ubiquitination site in the DBD necessary for the ubiquitination degradation [Wadosky and Willis, 2012]. Like PPAR β/δ, the Nr1d1 may have the ubiquitination site for protein degradation in the DBD, so the deletion of the DBD in Nr1d1 might block the proteasomal degradation. It is just a hypothesis, and further study is required for the degradation of the Nr1d1.

The overexpressed and truncated mutant protein has no nuclear activity for the RevRE as a transcriptional factor, and did not reverse the transcriptional repression by the Nr1d1 WT (Figure 13-15). Of note, the Nr1d1 Δex3/4 has no dominant-negative activity on the classical RevRE. Thus, this strategy is valid for the study of the functions and roles in the Nr1d1.

4.3. Experimental model of NAFLD in the Nr1d1 Δex3/4 mice

Animal models in which single genes are targeted have contributed to the understanding of human diseases, but there are phenotypic discrepancies between available animal models and human diseases in many cases. These discrepancies are particularly marked for NAFLD and NASH because the causes of these diseases are complex and involve interplay between genetic and environmental factors [Day, 2002]. To overcome these problems, many experiments employ a combination of animal models of genetic mutation and imbalanced nutritional diets in the investigation of NAFLD [Takahashi et al., 2012]. Substantially, the use of an HFD is considered a primary cause of the development of NAFLD. Many studies in rodent models have demonstrated that HFD feeding induces hepatic steatosis accompanied by the retention of TGs synthesized in the liver [Lieber et al., 2004; Biddinger et al., 2005; Zou et al., 2006]. These diets model resemble human NAFLD in that total dietary fat intake is strongly associated with hepatic fat content [Westerbacka et al., 2005; Cortez-Pinto et al., 2006; Wehmeyer et al., 2016].

In the present study, genetically modified mice lacking exons 3 and 4 encoding the DBD of the *Nr1d1* gene were challenged with a HFD. Although the deletion of the DBD produced no changes in hepatic phenotype compared with the WT mice after LFD feeding, the Nr1d1 Δex3/4 mice showed significantly enhanced histological and metabolic hepatic steatosis (Figure 19,

22 and 23). The aim of this study was to examine the contribution of the Nr1d1 to the physiological effect of HFD by evaluating the hepatic phenotype of the Nr1d1 Δex3/4 mice. In the context of fatty liver disease, nutrition challenges such as HFD and high carbohydrate diet are the important factors that have a reflection of uncontrolled metabolism status to the liver health. As such, this study provides evidences that the function of DBD for Nr1d1 as an empirical modifier of hepatic lipid metabolism in the pathogenesis of NAFLD. This animal model also supports the concept of genetic–environmental interactions in that different genotypes respond differently to different environments [Plomin et al., 1977].

As NAFLD is thought to be resulted from complex metabolic diseases, specific dietary challenges have limitation not to copy various conditions of fatty liver diseases. In addition to HFD feeding, there are many dietary and chemical models for NAFLD, such as methionine and choline deficiency (MCD) diet, high fructose diet, atherogenic diet (high cholesterol and cholate diet), and drugs [Takahashi et al., 2012]. Using theses dietary models, chronic metabolic disease statuses like obesity and insulin resistance are controlled for aim of study. Thus, the Nr1d1 Δex3/4 mice model should be examined with various dietary and chemical challenges to be responsible to hepatic lipid metabolism.

4.4. Understanding the pathophysiological meaning of gene set affected by interaction effect

The gene expression profiling shown in Figure 31 and 32 further demonstrates the interaction of genotype and diet in the HFD-fed Nr1d1 Δex3/4 mice. The number of differentially expressed genes for the interaction effect was similar to that of the diet effect, suggesting that these genes might explain the enhancement of hepatic steatosis observed in the HFD-fed Nr1d1 Δex3/4 mice. The biological processes enriched by the differentially expressed genes for these interactions included neutrophil homeostasis and cyclic adenosine monophosphate (cAMP) metabolism (Table 5).

The hepatic accumulation of neutrophils is prominent in cases of NAFLD and NASH, and recruitment of neutrophils to inflamed sites is induced by various cytokines and chemokines including interleukin 17 (IL-17) [Xu et al., 2014]. Intriguingly, Nr1d1 was reported to regulate the differentiation of IL-17-producing CD4+ T helper cells, Th17, in a diurnal manner [Yu et al., 2013]. Thus, cooperation of Th17 cells with the hepatic gene products of the interaction effect might contribute to the neutrophil homeostasis that is involved in hepatic steatosis of the HFD-fed Nr1d1 Δex3/4 mice.

On the other hand, cAMP is a crucial secondary messenger that induces signal transduction pathways associated with very-low-density lipoprotein secretion, lipogenesis, and lipid import to the liver [Björnsson et al., 1994; Lu and Shyy,

2006; Zingg et al., 2016]. Because cAMP signaling is regulated rhythmically by a circadian clock system and it controls the expression as well as transactivation of Nr1d1, cAMP metabolism might play a critical role in connecting the genotypic and dietary effects in this mouse model [Downes et al., 1995; O'Neill et al., 2008].

Taken together, further studies are needed to elucidate a clear link between these biological processes and the function of Nr1d1 in the pathogenesis of NFALD.

4.5. Non-classical functions of the Nr1d1 in hepatic lipid metabolism

Here, an anti-steatogenic function of Nr1d1 using a mutant mouse lacking transcriptional repression was defined. However, this function may be associated with a high level of expression of the internally truncated Nr1d1 (Figures 10-12). Although the Nr1d1 mutant lacking the DBD lost DNA binding and subsequent transcription, the mutant protein might retain a nonclassical function mediated by protein–protein interactions. Because the activation function domain and the ligand-binding domain serve as interfaces for protein–protein interaction, the Nr1d1 mutant protein might retain its ability to respond to specific interactions in response to HFD feeding [Everett et al., 2014]. Of interest, cistromic studies have revealed that enriched motifs

of *in vivo* Nr1d1 binding sites included other DNA binding site regions of transcriptional factors such as peroxisome proliferator-activated receptor gamma, Hnf4/6, Cebp, and estrogen-related receptor alpha in addition to the classical Nr1d1 binding sites [Cho et al., 2012; Zhang et al., 2015]. Thus, the result from our TFBS enrichment analysis could provide a hint for the molecular mechanism of the enhanced hepatic steatosis in the HFD-fed Nr1d1 Δex3/4 mice, in that Cebpα and Hnf4α, the upstream regulators identified, might act as effectors for the nonclassical function of Nr1d1 (Figures 33 and 34).

One of the common downstream targets of both Cebpα and Hnf4α is *Thrsp*, the expression of which was associated with the genetic, diet, and interaction effects (Figure 31). Up to recent, the roles of Thrsp in the liver have been proposed to regulate *de novo* lipogenesis by diets and hormones [Brown et al., 1997; Aipoalani et al., 2010; Wu et al., 2013]. To deeply understand functions and roles of Thrsp, the coexpressed gene network with Thrsp was analyzed in the liver network using Cytopscape plug-in GeneMANIA application [Crumbley et al., 2011]. The coexpressed genes are significantly annotated with the terms "Generation of precursor metabolites and energy". It is consistent with the phenotypic change of hepatic steatosis in the mice. These data suggested that *Thrsp* is a putative target gene of Nr1d1 in hepatic lipid metabolism on the pathogenesis of NAFLD.

The relative contribution of the classical function versus the nonclassical

function of the Nr1d1 in hepatic lipid metabolism could be assessed in the future by employing other genetic mutant mouse models with whole *Nr1d1* gene deletions.

4.6. The discrepancies of hepatic steatosis phenotypes between the whole-body and liver-specific Nr1d1 Δex3/4 mice

The discrepancies of hepatic steatosis between the whole-body and liver-specific mutant mice were first resulted from the difference of susceptibility for HFD-induced obesity. While the Nr1d1 Δex3/4 mice were responsible to HFD-induced obesity, the Nr1d1 LΔex3/4 mice did not distinguish the response from the Nr1d1 Fl/Fl mice. As well, body weights, histological status, and fatty liver status of the Nr1d1 LΔex3/4 mice were the same to the Nr1d1 Fl/Fl mice. It is thought that the Nr1d1 gene ablation in the liver alone did not recapitulate the metabolic dysfunction observed in the whole-body Nr1d1 Δex3/4 mice, suggesting that the Nr1d1 may exert metabolic control, in part, through effects in other tissues such as adipose tissues and the central nervous system. The Sirt3 gene is a similar example. Sirt3 germline knockout mice develop obesity, insulin resistance, and hepatic steatosis in response to a HFD challenge [Hirschey et al., 2011]. Incidentally, Sirt3 skeletal muscle-specific or liver-specific knockout mice display no changed phenotype [Fernandez-Marcos et al., 2012; Lombard and Zwaans, 2014].

To overcome the discrepancies and investigate the interactive tissues for the liver in the action of the Nr1d1, the incorporation of multiple *in vivo* Cre recombinations is available. In other words, the problem can be solved by crossing the Nr1d1 Fl/Fl mice with multiple Cre mice and generating multiple tissue deleted mice models. It was reported that Scd1 liver-specific knockout mice, unlike the systemic knockout mice, were not protected from HFD-induced obesity [Miyazaki et al., 2007]. It is because inhibition of liver SCD1 alone is insufficient to elicit the hypermetabolism and increased energy expenditure necessary to compensate for the increased energy intake associated with HFD feeding. However, double tissues knockout mice from adipose tissues and liver showed decreased free fatty acid composition, supporting the existence of extensive lipid cross-talk between liver and adipose tissue [Flowers et al., 2012]. Thus, multiple tissue-specific knockout mice in the Nr1d1 help to understand the hepatic lipid metabolism.

5. Conclusion

The results of this thesis can be summarized as follows:

Targeted disruption of the Nr1d1 exons 3 and 4 resulted in a DBD-deleted mutant mouse. Although the Nr1d1 Δex3/4 mutant protein was overexpressed in the cells, and partially expressed in the nucleus, it does not have direct transcriptional activity. Hepatic steatosis in the Nr1d1 Δex3/4 mice was deteriorated compared to the Nr1d1 WT mice after HFD feeding, indicating an interaction between diet and genotype for this phenotypic change. Gene expression profiling revealed that the interaction between diet and genotype might involve neutrophil recruitment and the cAMP metabolic pathway, and be associated with the liver-enriched metabolic transcriptional factors, Cebpα and Hnf4α as upstream regulators. *Thrsp*, which expression was altered by the interaction effect, was predicted to coexpress with the genes associated with fatty acid metabolism, suggested to be a potential target gene of the Nr1d1 in NAFLD. Therefore, loss of DNA bidning of Nr1d1 was significantly associated with worsened hepatic steatosis. The interaction between the *Nr1d1* Δex3/4 genotype and HFD might mediate these phenotypic changes, probably through a nonclassical transcriptional function of Nr1d1.

Bibliography

Achermann JC, Jameson JL (2003) Human disorders caused by nuclear receptor gene mutatinos. Pure Appl Chem 75:1785-1796.

Adelmant G, Bègue A, Stéhelin D, Laudet V (1996) A functional Rev-erb alpha responsive element located in the human Rev-erb alpha promoter mediates a repressing activity. Proc Natl Acad Sci U S A 93:3553-3558.

Aipoalani DL, O'Callaghan BL, Mashek DG, Mariash CN, Towle HC (2010) Overlapping roles of the glucose-responsive genes, S14 and S14R, in hepatic lipogenesis. Endocrinology 151:2071-2077.

Armstrong MJ, Adams LA, Canbay A, Syn WK (2014) Extrahepatic complications of nonalcoholic fatty liver disease. Hepatology 59:1174-1197.

Bechmann LP, Hannivoort RA, Gerken G, Hotamisligil GS, Trauner M, Canbay A (2012) The interaction of hepatic lipid and glucose metabolism in liver diseases. J Hepatol 56:952-964.

Biddinger SB, Almind K, Miyazaki M, Kokkotou E, Ntambi JM, Kahn CR (2005) Effects of diet and genetic background on sterol regulatory element-binding protein-1c, stearoyl-CoA desaturase 1, and the development of the metabolic syndrome. Diabetes 54:1314-1323.

Björnsson OG, Sparks JD, Sparks CE, Gibbons GF (1994) Regulation of VLDL secretion in primary culture of rat hepatocytes: involvement of cAMP and cAMP-dependent protein kinases. Eur J Clin Invest 24:137-148.

Brown SB, Maloney M, Kinlaw WB (1997) "Spot 14" protein functions at the pretranslational level in the regulation of hepatic metabolism by thyroid hormone and glucose. J Biol Chem 272:2163-2166.

Bugge A, Feng D, Everett LJ, Briggs ER, Mullican SE, Wang F, Jager J, Lazar MA (2012) Rev-erbα and Rev-erbβ coordinately protect the

circadian clock and normal metabolic function. Genes Dev 26:657-667.

Cave MC, Clair HB, Hardesty JE, Falkner KC, Feng W, Clark BJ, Sidey J, Shi H, Aqel BA, McClain CJ, Prough RA (2016) Nuclear receptors and nonalcoholic fatty liver disease. Biochim Biophys Acta 1859:1083-1099.

Cho H, Zhao X, Hatori M, Yu RT, Barish GD, Lam MT, Chong LW, DiTacchio L, Atkins AR, Glass CK, Liddle C, Auwerx J, Downes M, Panda S, Evans RM (2012) Regulation of circadian behaviour and metabolism by REV-ERB-α and REV-ERB-β. Nature 485:123-127.

Chawla A, Lazar MA (1993) Induction of Rev-ErbA alpha, an orphan receptor encoded on the opposite strand of the alpha-thyroid hormone receptor gene, during adipocyte differentiation. J Biol Chem 268:16265-16269.

Chen J, Bardes EE, Aronow BJ, Jegga AG (2009) ToppGene Suite for gene list enrichment analysis and candidate gene prioritization. Nucleic Acids Res 37:W305-W311.

Chomez P, Neveu I, Mansén A, Kiesler E, Larsson L, Vennström B, Arenas E (2000) Increased cell death and delayed development in the cerebellum of mice lacking the rev-erbA(alpha) orphan receptor. Development 127:1489-1498.

Chopin-Delannoy S, Thénot S, Delaunay F, Buisine E, Begue A, Duterque-Coquillaud M, Laudet V (2003) A specific and unusual nuclear localization signal in the DNA binding domain of the Rev-erb orphan receptors. J Mol Endocrinol 30:197-211.

Cohen JC, Horton JD, Hobbs HH (2011) Human fatty liver disease: old questions and new insights. Science 332:1519-1523.

Cortez-Pinto H, Jesus L, Barros H, Lopes C, Moura MC, Camilo ME (2006) How different is the dietary pattern in non-alcoholic steatohepatitis patients? Clin Nutr 25:816-823.

Crumbley C, Wang Y, Kojetin DJ, Burris TP (2010) Characterization of the core mammalian clock component, NPAS2, as a REV-ERBalpha /

RORalpha target gene. J Biol Chem 285:35386-35392.

Crumbley C, Burris TP (2011) Direct regulation of CLOCK expression by REV-ERB. PLoS One 6:e17290.

Day CP (2002) Pathogenesis of steatohepatitis. Best Pract Res Clin Gastroenterol 16:663-678.

Delezie J, Dumont S, Dardente H, Oudart H, Gréchez-Cassiau A, Klosen P, Teboul M, Delaunay F, Pévet P, Challet E (2012) The nuclear receptor REV-ERBα is required for the daily balance of carbohydrate and lipid metabolism. FASEB J 26:3321-3335.

Downes M, Carozzi AJ, Muscat GE (1995) Constitutive expression of the orphan receptor, Rev-erbA alpha, inhibits muscle differentiation and abrogates the expression of the myoD gene family. Mol Endocrinol 9:1666-1678.

Duez H, van der Veen JN, Duhem C, Pourcet B, Touvier T, Fontaine C, Derudas B, Baugé E, Havinga R, Bloks VW, Wolters H, van der Sluijs FH, Vennström B, Kuipers F, Staels B (2008) Regulation of bile acid synthesis by the nuclear receptor Rev-erbalpha. Gastroenterology 135:689-698.

Everett LJ, Lazar MA (2014) Nuclear receptor Rev-erbα: up, down, and all around. Trends Endocrinol Metab 25:586-592.

Fernandez-Marcos PJ, Jeninga EH, Canto C, Harach T, de Boer VC, Andreux P, Moullan N, Pirinen E, Yamamoto H, Houten SM, Schoonjans K, Auwerx J (2012) Muscle or liver-specific Sirt3 deficiency induces hyperacetylation of mitochondrial proteins without affecting global metabolic homeostasis. Sci Rep 2:425.

Flowers MT, Ade L, Strable MS, Ntambi JM (2012) Combined deletion of SCD1 from adipose tissue and liver does not protect mice from obesity. J Lipid Res 53:1646-1653.

Fontaine C, Dubois G, Duguay Y, Helledie T, Vu-Dac N, Gervois P, Soncin F, Mandrup S, Fruchart JC, Fruchart-Najib J, Staels B (2003) The orphan

nuclear receptor Rev-Erbalpha is a peroxisome proliferator-activated receptor (PPAR) gamma target gene and promotes PPARgamma-induced adipocyte differentiation. J Biol Chem 278:37672-37680.

Fontaine C, Rigamonti E, Pourcet B, Duez H, Duhem C, Fruchart JC, Chinetti-Gbaguidi G, Staels B (2008) The nuclear receptor Rev-erbalpha is a liver X receptor (LXR) target gene driving a negative feedback loop on select LXR-induced pathways in human macrophages. Mol Endocrinol 22:1797-1811.

Forman BM, Chen J, Blumberg B, Kliewer SA, Henshaw R, Ong ES, Evans RM (1994) Cross-talk among ROR alpha 1 and the Rev-erb family of orphan nuclear receptors. Mol Endocrinol 8:1253-1261.

Gerhart-Hines Z, Feng D, Emmett MJ, Everett LJ, Loro E, Briggs ER, Bugge A, Hou C, Ferrara C, Seale P, Pryma DA, Khurana TS, Lazar MA (2013) The nuclear receptor Rev-erbα controls circadian thermogenic plasticity. Nature 503:410-413.

Gibbs JE, Blaikley J, Beesley S, Matthews L, Simpson KD, Boyce SH, Farrow SN, Else KJ, Singh D, Ray DW, Loudon AS (2012) The nuclear receptor REV-ERBα mediates circadian regulation of innate immunity through selective regulation of inflammatory cytokines. Proc Natl Acad Sci U S A 109:582-587.

Han YH, Kim HJ, Kim EJ, Kim KS, Hong S, Park HG, Lee MO (2014) RORα decreases oxidative stress through the induction of SOD2 and GPx1 expression and thereby protects against nonalcoholic steatohepatitis in mice. Antioxid Redox Signal 21:2083-2094.

Harding HP, Lazar MA (1993) The orphan receptor Rev-ErbA alpha activates transcription via a novel response element. Mol Cell Biol 13:3113-3121.

Harding HP, Lazar MA (1995) The monomer-binding orphan receptor Rev-Erb represses transcription as a dimer on a novel direct repeat. Mol Cell Biol 15: 4791-4802.

Hardy T, Oakley F, Anstee QM, Day CP (2016) Nonalcoholic Fatty Liver Disease: Pathogenesis and Disease Spectrum. Annu Rev Pathol 11:451-496.

Hayhurst GP, Lee YH, Lambert G, Ward JM, Gonzalez FJ (2001) Hepatocyte nuclear factor 4alpha (nuclear receptor 2A1) is essential for maintenance of hepatic gene expression and lipid homeostasis. Mol Cell Biol 21:1393-1403.

Hirschey MD, Shimazu T, Jing E, Grueter CA, Collins AM, Aouizerat B, Stančáková A, Goetzman E, Lam MM, Schwer B, Stevens RD, Muehlbauer MJ, Kakar S, Bass NM, Kuusisto J, Laakso M, Alt FW, Newgard CB, Farese RV Jr, Kahn CR, Verdin E (2011) SIRT3 deficiency and mitochondrial protein hyperacetylation accelerate the development of the metabolic syndrome. Mol Cell 44:177-190.

Isayama K, Zhao L, Chen H, Yamauchi N, Shigeyoshi Y, Hashimoto S, Hattori MA (2015) Removal of Rev-erbα inhibition contributes to the prostaglandin G/H synthase 2 expression in rat endometrial stromal cells. Am J Physiol Endocrinol Metab 308:E650-E661.

Jeon Y, Ko E, Lee KY, Ko MJ, Park SY, Kang J, Jeon CH, Lee H, Hwang DS (2011) TopBP1 Deficiency Causes an Early Embryonic Lethality and Induces Cellular Senescence in Primary Cells. J Biol Chem 286:5414–5422.

Kim EJ, Yoon YS, Hong S, Son HY, Na TY, Lee MH, Kang HJ, Park J, Cho WJ, Kim SG, Koo SH, Park HG, Lee MO (2012) Retinoic acid receptor-related orphan receptor α-induced activation of adenosine monophosphate-activated protein kinase results in attenuation of hepatic steatosis. Hepatology 55:1379-1388.

Kojetin DJ, Burris TP (2014) REV-ERB and ROR nuclear receptors as drug targets. Nat Rev Drug Discov 13:197-216.

Kornmann B, Schaad O, Bujard H, Takahashi JS, Schibler U (2007) System-driven and oscillator-dependent circadian transcription in mice with a

conditionally active liver clock. PLoS Biol 5:e34.

Kwon AT, Arenillas DJ, Worsley Hunt R, Wasserman WW (2012) oPOSSUM-3: advanced analysis of regulatory motif over-representation across genes or ChIP-Seq datasets. G3-Genes Genomes Genet 2:987-1002.

Lam MT, Cho H, Lesch HP, Gosselin D, Heinz S, Tanaka-Oishi Y, Benner C, Kaikkonen MU, Kim AS, Kosaka M, Lee CY, Watt A, Grossman TR, Rosenfeld MG, Evans RM, Glass CK (2013) Rev-Erbs repress macrophage gene expression by inhibiting enhancer-directed transcription. Nature 498:511-515.

Lassailly G, Caiazzo R, Pattou F, Mathurin P (2016) Perspectives on Treatment for Nonalcoholic Steatohepatitis. Gastroenterology 150:1835-1848.

Lazar MA, Hodin RA, Darling DS, Chin WW (1989) A novel member of the thyroid/steroid hormone receptor family is encoded by the opposite strand of the rat c-erbA alpha transcriptional unit. Mol Cell Biol 9:1128-1136.

Lazar MA, Jones KE, Chin WW (1990) Isolation of a cDNA encoding human Rev-ErbA alpha: transcription from the noncoding DNA strand of a thyroid hormone receptor gene results in a related protein that does not bind thyroid hormone. DNA Cell Biol 9:77-83.

Le Martelot G, Claudel T, Gatfield D, Schaad O, Kornmann B, Lo Sasso G, Moschetta A, Schibler U (2009) REV-ERBalpha participates in circadian SREBP signaling and bile acid homeostasis. PLoS Biol 7:e1000181.

Lee MH, Hong I, Kim M, Lee BH, Kim JH, Kang KS, Kim HL, Yoon BI, Chung H, Kong G, Lee MO (2008) Gene expression profiles of murine fatty liver induced by the administration of methotrexate. Toxicology 249:75-84.

Lee MH, Na H, Kim EJ, Lee HW, Lee MO (2012) Poly(ADP-ribosyl)ation of p53 induces gene-specific transcriptional repression of MTA1.

Oncogene 31:5099-5107.

Lee DH, Park JO, Kim TS, Kim SK, Kim TH, Kim MC, Park GS, Kim JH, Kuninaka S, Olson EN, Saya H, Kim SY, Lee H, Lim DS (2016) LATS-YAP/TAZ controls lineage specification by regulating TGFβ signaling and Hnf4α expression during liver development. Nat Commun 7:11961.

Lewandoski M, Wassarman KM, Martin GR (1997) Zp3-cre, a transgenic mouse line for the activation or inactivation of loxP-flanked target genes specifically in the female germ line. Curr Biol 7:148-151.

Li T, Eheim AL, Klein S, Uschner FE, Smith AC, Brandon-Warner E, Ghosh S, Bonkovsky HL, Trebicka J, Schrum LW (2014) Novel role of nuclear receptor Rev-erbα in hepatic stellate cell activation: potential therapeutic target for liver injury. Hepatology 59:2383-2396.

Li X, Xu M, Wang F, Kohan AB, Haas MK, Yang Q, Lou D, Obici S, Davidson WS, Tso P (2014) Apolipoprotein A-IV reduces hepatic gluconeogenesis through nuclear receptor NR1D1. J Biol Chem 289:2396-2404.

Lieber CS, Leo MA, Mak KM, Xu Y, Cao Q, Ren C, Ponomarenko A, DeCarli LM (2004) Model of nonalcoholic steatohepatitis. Am J Clin Nutr 79:502-509.

Livak KJ, Schmittgen TD (2001) Analysis of relative gene expression data using real-time quantitative PCR and the 2(-Delta Delta C(T)) Method. Methods 25:402-408.

Lombard DB, Zwaans BM (2014) SIRT3: as simple as it seems? Gerontology 60:56-64.

López-Velázquez JA, Carrillo-Córdova LD, Chávez-Tapia NC, Uribe M, Méndez-Sánchez N (2012) Nuclear receptors in nonalcoholic Fatty liver disease. J Lipids 2012:139875.

Lu M, Shyy JY (2006) Sterol regulatory element-binding protein 1 is negatively modulated by PKA phosphorylation. Am J Physiol Cell Physiol 290:C1477-C1486.

Ma H, Zhong W, Jiang Y, Fontaine C, Li S, Fu J, Olkkonen VM, Staels B, Yan D (2013) Increased atherosclerotic lesions in LDL receptor deficient mice with hematopoietic nuclear receptor Rev-erbα knock- down. J Am Heart Assoc 2:e000235.

Marciano DP, Chang MR, Corzo CA, Goswami D, Lam VQ, Pascal BD, Griffin PR (2014) The therapeutic potential of nuclear receptor modulators for treatment of metabolic disorders: PPARγ, RORs, and Rev-erbs. Cell Metab 19:193-208.

Miyajima N, Horiuchi R, Shibuya Y, Fukushige S, Matsubara K, Toyoshima K, Yamamoto T (1989) Two erbA homologs encoding proteins with different T3 binding capacities are transcribed from opposite DNA strands of the same genetic locus. Cell 57: 31-39.

Miyazaki M, Flowers MT, Sampath H, Chu K, Otzelberger C, Liu X, Ntambi JM (2007) Hepatic stearoyl-CoA desaturase-1 deficiency protects mice from carbohydrate-induced adiposity and hepatic steatosis. Cell Metab 6:484-496.

Nam D, Chatterjee S, Yin H, Liu R, Lee J, Yechoor VK, Ma K (2015) Novel Function of Rev-erbα in Promoting Brown Adipogenesis. Sci Rep 5:11239.

Norris AW, Chen L, Fisher SJ, Szanto I, Ristow M, Jozsi AC, Hirshman MF, Rosen ED, Goodyear LJ, Gonzalez FJ, Spiegelman BM, Kahn CR (2003) Muscle-specific PPARgamma-deficient mice develop increased adiposity and insulin resistance but respond to thiazolidinediones. J Clin Invest 112:608-618.

O'Neill JS, Maywood ES, Chesham JE, Takahashi JS, Hastings MH (2008) cAMP-dependent signaling as a core component of the mammalian circadian pacemaker. Science 320:949-953.

Paglialunga S, Dehn CA (2016) Clinical assessment of hepatic de novo lipogenesis in non-alcoholic fatty liver disease. Lipids Health Dis 15:159.

Pawlak M, Lefebvre P, Staels B (2012) General molecular biology and

architecture of nuclear receptors. Curr Top Med Chem 12:486-504.

Pircher P, Chomez P, Yu F, Vennström B, Larsson L (2005) Aberrant expression of myosin isoforms in skeletal muscles from mice lacking the rev-erbAalpha orphan receptor gene. Am J Physiol Regul Integr Comp Physiol 288:R482-R490.

Plomin R, DeFries JC, Loehlin JC (1977) Genotype-environment interaction and correlation in the analysis of human behavior. Psychol Bull 84:309-322.

Porter C, Cohen NH (1996) Indirect calorimetry in critically ill patients: role of the clinical dietitian in interpreting results. J Am Diet Assoc 96:49-57.

Preitner N, Damiola F, Lopez-Molina L, Zakany J, Duboule D, Albrecht U, Schibler U (2002) The orphan nuclear receptor REV-ERBalpha controls circadian transcription within the positive limb of the mammalian circadian oscillator. Cell 110:251-260.

Raghuram S, Stayrook KR, Huang P, Rogers PM, Nosie AK, McClure DB, Burris LL, Khorasanizadeh S, Burris TP, Rastinejad F (2007) Identification of heme as the ligand for the orphan nuclear receptors REV-ERBalpha and REV-ERBbeta. Nat Struct Mol Biol 14:1207-1213.

Ramji DP, Foka P (2002) CCAAT/enhancer-binding proteins: structure, function and regulation. Biochem J 365:561-575.

Raspé E, Duez H, Mansén A, Fontaine C, Fiévet C, Fruchart JC, Vennström B, Staels B (2002) Identification of Rev-erbalpha as a physiological repressor of apoC-III gene transcription. J Lipid Res 43:2172-2179.

Sato S, Sakurai T, Ogasawara J, Takahashi M, Izawa T, Imaizumi K, Taniguchi N, Ohno H, Kizaki T (2014) A circadian clock gene, Rev-erbα, modulates the inflammatory function of macrophages through the negative regulation of Ccl2 expression. J Immunol 192:407-417.

Schmutz I, Ripperger JA, Baeriswyl-Aebischer S, Albrecht U (2010) The mammalian clock component PERIOD2 coordinates circadian output by interaction with nuclear receptors. Genes Dev 24:345-357.

Szczepaniak LS, Nurenberg P, Leonard D, Browning JD, Reingold JS, Grundy S, Hobbs HH, Dobbins RL (2005) Magnetic resonance spectroscopy to measure hepatic triglyceride content: prevalence of hepatic steatosis in the general population. Am J Physiol Endocrinol Metab 288:E462-E468.

Takahashi Y, Soejima Y, Fukusato T (2012) Animal models of nonalcoholic fatty liver disease/nonalcoholic steatohepatitis. World J Gastroenterol 18:2300-2308.

Tsochatzis EA, Bosch J, Burroughs AK (2014) Liver cirrhosis. Lancet 383:1749-1761.

Wadosky KM, Willis MS (2012) The story so far: post-translational regulation of peroxisome proliferator-activated receptors by ubiquitination and SUMOylation. Am J Physiol Heart Circ Physiol 302:H515-H526.

Wagner M, Zollner G, Trauner M (2011) Nuclear receptors in liver disease. Hepatology 53:1023-1034.

Wang J, Lazar MA (2008) Bifunctional role of Rev-erbalpha in adipocyte differentiation. Mol Cell Biol 28:2213-2220.

Warde-Farley D, Donaldson SL, Comes O, Zuberi K, Badrawi R, Chao P, Franz M, Grouios C, Kazi F, Lopes CT, Maitland A, Mostafavi S, Montojo J, Shao Q, Wright G, Bader GD, Morris Q (2010) The GeneMANIA prediction server: biological network integration for gene prioritization and predicting gene function. Nucleic Acids Res 38:W214-W220.

Wehmeyer MH, Zyriax BC, Jagemann B, Roth E, Windler E, Schulze Zur Wiesch J, Lohse AW, Kluwe J (2016) Nonalcoholic fatty liver disease is associated with excessive calorie intake rather than a distinctive dietary pattern. Medicine (Baltimore) 95:e3887.

Westerbacka J, Lammi K, Häkkinen AM, Rissanen A, Salminen I, Aro A, Yki-Järvinen H (2005) Dietary fat content modifies liver fat in

overweight nondiabetic subjects. J Clin Endocrinol Metab 90:2804-2809.

Woldt E, Sebti Y, Solt LA, Duhem C, Lancel S, Eeckhoute J, Hesselink MK, Paquet C, Delhaye S, Shin Y, Kamenecka TM, Schaart G, Lefebvre P, Nevière R, Burris TP, Schrauwen P, Staels B, Duez H (2013) Rev-erb-α modulates skeletal muscle oxidative capacity by regulating mitochondrial biogenesis and autophagy. Nat Med 19:1039-46.

Wu J, Wang C, Li S, Li S, Wang S, Li J, Chi Y, Yang H, Kong X, Zhou Y, Dong C, Wang F, Xu G, Yang J, Gustafsson JÅ , Guan Y (2013) Thyroid hormone-responsive SPOT 14 homolog promotes hepatic lipogenesis, and its expression is regulated by liver X receptor α through a sterol regulatory element-binding protein 1c-dependent mechanism in mice. Hepatology 58:617-628.

Xu R, Huang H, Zhang Z, Wang FS (2014) The role of neutrophils in the development of liver diseases. Cell Mol Immunol 11:224-231.

Yamamoto T, Nakahata Y, Soma H, Akashi M, Mamine T, Takumi T (2004) Transcriptional oscillation of canonical clock genes in mouse peripheral tissues. BMC Mol Biol 5:18.

Yin L, Lazar MA (2005) The orphan nuclear receptor Rev-erbalpha recruits the N-CoR/histone deacetylase 3 corepressor to regulate the circadian Bmal1 gene. Mol Endocrinol 19:1452-1459.

Yin L, Wu N, Curtin JC, Qatanani M, Szwergold NR, Reid RA, Waitt GM, Parks DJ, Pearce KH, Wisely GB, Lazar MA (2007) Rev-erbalpha, a heme sensor that coordinates metabolic and circadian pathways. Science 318:1786-1789.

Yoo YG, Na TY, Seo HW, Seong JK, Park CK, Shin YK, Lee MO (2008) Hepatitis B virus X protein induces the expression of MTA1 and HDAC1, which enhances hypoxia signaling in hepatocellular carcinoma cells. Oncogene 27:3405-3013.

Younossi ZM, Koenig AB, Abdelatif D, Fazel Y, Henry L, Wymer M (2016) Global epidemiology of nonalcoholic fatty liver disease-Meta-analytic

assessment of prevalence, incidence, and outcomes. Hepatology 64:73-84.

Yu W, Nomura M, Ikeda M (2002) Interactivating feedback loops within the mammalian clock: BMAL1 is negatively autoregulated and upregulated by CRY1, CRY2, and PER2. Biochem Biophys Res Commun 290:933-941.

Yu X, Rollins D, Ruhn KA, Stubblefield JJ, Green CB, Kashiwada M, Rothman PB, Takahashi JS, Hooper LV (2013) TH17 cell differentiation is regulated by the circadian clock. Science 342:727-730.

Zhang Y, Fang B, Emmett MJ, Damle M, Sun Z, Feng D, Armour SM, Remsberg JR, Jager J, Soccio RE, Steger DJ, Lazar MA (2015) GENE REGULATION. Discrete functions of nuclear receptor Rev-erbα couple metabolism to the clock. Science 348:1488-1492.

Zingg JM, Hasan ST, Nakagawa K, Canepa E, Ricciarelli R, Villacorta L, Azzi A, Meydani M (2016) Modulation of cAMP levels by high-fat diet and curcumin and regulatory effects on CD36/FAT scavenger receptor / fatty acids transporter gene expression. Biofactors.

Zou Y, Li J, Lu C, Wang J, Ge J, Huang Y, Zhang L, Wang Y (2006) High-fat emulsion-induced rat model of nonalcoholic steatohepatitis. Life Sci 79:1100-1107.

초 록

지방간질환에서 핵수용체 NR1D1의 병태생리학적 역할에 대한 연구

서울대학교 대학원
약학과 병태생리학 전공
나혜린

복합적인 원인에 의해 발병하는 지방간질환의 연구에 있어 약물 타깃으로서 유용한 핵 수용체 분야의 연구가 활발히 진행되고 있다. 핵수용체 NR1D1은 생체 내 에너지 대사 항상성에 기여하는 지방조직, 간, 골격근 등과 같은 다양한 조직과 간성상세포, 대식세포, 면역세포 등과 같은 특이적 세포에서 과발현 하고, 지방세포형성, 골격근 형성, 염증, 면역 반응 등에 관여하고 있는 것으로 밝혀져 왔다. 그러나 지방간질환 발병과 기전에 있어 분명히 그 역할이 언급되지 못 하고 있다. 지방간질환의 발병에서 핵수용체 NR1D1의 기능과 역할을 규명하기 위해, DNA 결합 부위를 코딩하는 엑손 3과 4 부위가 제거된 Nr1d1 유전자 변형 (Nr1d1 Δex3/4) 마우스에 고지방식이를 적용하여 지방간 형성을 유도하였다. 고지방식이에 의해 Nr1d1 Δex3/4 마우스는 정상 마우스에 대비하여 조직학적으로 간세포에 지질에 축적되어 있고, 조직 내에서 검출한 중성지방이 유의적으로 증가되어 지방간이 심화되었다. 간 손상 지표인 AST와 ALT 수치가 유의적으로 증가되어 있음을 확인함으로써, 간 손상까

지 동반된 상태임을 알 수 있었다. 이러한 형질적인 변화에 대해, 마이크로어레이를 통해 유전자 발현 양상을 확인하여 본 결과, 고지방식이와 유전자형의 상호작용에 의해 호중구 항상성과 cAMP 신호계에 관련된 기능적인 네트워크와 관련된 유전자들의 발현이 유의적으로 변화하여, 심화된 지방간 형성에 기여하고 있음을 알 수 있었다. Nr1d1 Δex3/4는 Nr1d1의 DNA 결합능이 결여되어 있기 때문에 전사를 직접적으로 조절하기 어려울 것이라 예상되었다. 그래서 유의적인 발현 변화를 보인 유전자들을 조절하는 분자적 기전에 대해 이해하기 위해, 상위 전사인자를 분석한 결과, CCAAT/enhancer-binding protein alpha (Cebpα)와 Hepatocyte nuclear factor 4 alpha (Hnf4α)이 작용하고 있음을 예측할 수 있었다. 이는 Nr1d1이 핵수용체로서 가지는 대안적인 전사 활성을 반영하는 것으로 생각된다. 아울러, 고지방식이에서 Nr1d1의 DNA 결합능 결여는 *Thyroid hormone-responsive* (*Thrsp*)의 전사 발현을 조절하고 있었고, 이것은 지방간 질환에 있어 Nr1d1의 잠재적인 타깃 유전자임을 시사하고 있다. 본 연구에서 엑손 3과 4의 결손으로 인한 Nr1d1의 고유한 DNA 결합능 손실은 지방간 형성의 실질적인 요인이 되는 고지방식이와 상호작용하여 지방간질환을 유발할 수 있다는 새로운 사실을 알 수 있었다. 또한, Nr1d1가 대안적인 전사 활성 경로를 통해 지방간질환의 발병 과정에 영향을 미칠 수 있는 가능성을 확인하였다.

주요어: 핵 수용체, Nr1d1, 지방간질환, Cebp*α*, Hnf4*α*, Thrsp

학 번: 2009-30461